Title
Soil water budgets for winter-cropped rice systems in the Sacramento Valley

Author
Berris, Helaine

Publication Date
2022

Peer reviewed|Thesis/dissertation

Soil water budgets for winter-cropped rice systems in the Sacramento Valley

By
HELAINE BERRIS
THESIS

Submitted in partial satisfaction of the requirements for the degree of

MASTER OF SCIENCE

in

Hydrologic Sciences

in the

OFFICE OF GRADUATE STUDIES

of the

UNIVERSITY OF CALIFORNIA

DAVIS

Approved:

Kosana Suvočarev

Samuel Sandoval Solis

Mallika Nocco

Committee in Charge

2022

Abstract

California faces complicated water challenges and increased drought that have put pressure on agricultural systems to cut back on water consumption. Responding to changes in water supply and improving adaptive capacity requires that knowledge and expertise be available to growers and water managers. Water budgets are useful tools that aid in evaluating availability, change, and sustainability of water resources, however water budget components can be difficult to measure due to complex heterogeneity and inherent environmental physical properties. Capturing changes in soil moisture (ΔS) in systems with high clay content soils is notoriously complicated due to interferences from shrink-swell potential and soil-sensor contact. Using winter-cropped, fallowed rice fields in the Sacramento Valley, CA as a case study, we explore water budgets as a tool to inform water management and ecological enhancement while simultaneously evaluating time domain reflectometry (TDR) soil sensors' ability to measure ΔS in clayey soils. We examined spatial and temporal patterns of water budget components for an irrigated winter crop, an unirrigated winter crop, and a fallow field. During the extremely dry conditions of the 2020-21 water year, the irrigated winter crop and fallow site had a similar seasonal ΔS, while the unirrigated winter crop had much greater soil water depletion. We found the TDR sensor overestimated the magnitude of ΔS during precipitation and irrigation events when compared to recorded precipitation and underestimated ΔS during dry periods when compared to manually collected soil cores, but adequately captured patterns of infiltration and saturation in the soil profile.

Contents

Introduction

Background

Climate change, droughts, shifts in precipitation patterns, groundwater depletion, and population growth are some of many pressures that threaten freshwater resources and the agricultural systems that depend on them (Douville et al. 2021). On a global scale, agriculture accounts for 70% of total water use and demand is expected to increase significantly over the next two decades (Boretti et al. 2019). There is growing concern around food system sustainability and security as changing climate, environment, and anthropogenic landscapes continue to present uncertainty for water supplies where they are critically needed. Conflict between food and water demand may be felt worldwide, however more severely at regional and local scales (Boretti et al. 2019). To adequately face these challenges, growers and water managers need system-specific technical information and expertise to improve mitigation and adaptation strategies (Iglesias et al. 2015). Established scientific methodologies combined with innovative tools and technology can provide insight on temporal and spatial distributions of water in agricultural systems. Specifically, capturing field-scale hydrologic patterns in particular crops can assist stakeholders in developing agricultural water management plans during water shortages.

Water budgets are valuable tools that can evaluate availability, change, and sustainability of water resources. Using the principle of conservation of mass, it can be determined that the change in water storage of a system is equal to the difference between the system's inputs and outputs in a given control volume during a set period of time (Healy et al. 2007). Such a mass-based model can be informative of water supply and demand, ecosystem health, chemical transport and more. In water resources planning and

management, water budgets are often used to understand the effects of anthropogenic and non-anthropogenic factors on the quantity and quality of water resources, helping to guide conservation projects and climate change adaption and mitigation strategies (Stanton et al. 2011; Healy et al. 2007). Water budget models are versatile and can be applied to a variety of spatial (i.e., whole basin, single field) and temporal scales (i.e., hourly, daily, multi-year). Here, we focus on field scale water budgets in agricultural systems (Fig 1) where an appropriate water budget is stated as:

$$Eq\ 1: \Delta S = P + I - ETc - RO - D$$

Where ΔS (mm) is change in soil moisture, I (mm) is irrigation, P (mm) is precipitation, ETc (mm) is crop evapotranspiration, RO (mm) is runoff, and D (mm) is deep percolation.

In-situ monitoring is often used to measure a majority of water budget components (WBCs) and unmonitored terms are calculated as the residual of *Eq 1* (Healy et al. 2007). In these models, it is assumed that the water budget closure (or quantity of water unaccounted for) is equal to 0. This assumption can be problematic in that the error of measured WBCs are assigned to the calculated variable. However, it is unlikely that all WBCs can be measured simultaneously, effectively, and timely (Safeeq et al. 2021; Pan et al. 2017). Estimation of a single WBC as the residual of the water budget is a commonly used scientific method and is simple, accurate, and sound when other WBCs can be measured with confidence (Gochis et al. 2000; Verstraeten et al. 2008; Wan et al. 2015; Zeleke et al. 2012).

ETc has been estimated successfully at global , regional, and local scales with various levels of accuracy using soil water budgets obtained from in-situ soil sensors and remote sensing (Verstraeten et al. 2008). In agricultural systems, ETc can be costly and

difficult to obtain through in-situ measurements but can be estimated from water budget and soil monitoring techniques (*Eq. 1*). Most soil water sensors are cheaper and have less complicated installation and monitoring than eddy covariance towers used to directly measure field scale ETc. Also, derivation of ETc from soil water budgets do not require additional meteorological inputs, aside from precipitation (Wan et al. 2015). Studies have shown that field scale water budget estimates of ETc have yielded reasonable quantification of actual ETc when compared to the FAO method using established crop coefficients (Gochis et al. 2000; Zeleke et al. 2012).

It is also valuable to examine each WBC independently to distinguish patterns and characteristics between systems, providing insight into the underlying assumptions of the water budget *(Eq 2*) (Safeeq et al. 2021; Joyce et al. 2002). This research looks particularly at ΔS, an important WBC to consider in agricultural systems because of heterogeneity and responsiveness to different farm management practices. Variability in soil physical properties, cropping patterns, and climatic conditions affect how much water is left in the soil after the growing season, and soil water retention/depletion can influence cropping and field management choices (IAEA 2008; Tsubo et al. 2015; Nocco et al. 2018; Pan et al. 2017; Gochis et al. 2000). For example, in semi-arid Mediterranean climates with cool, wet winters and hot, dry summers, water evaporates quickly from the soil surface during the summer growing season (Johnson et al. 2015; Baldocchi et al. 2019). Therefore, it is desirable for water to be conserved, or in surplus ($+\Delta S$), from the rainy season for future crop use and groundwater recharge (Douville et al. 2021). Soils with large volumes of water depletion ($-\Delta S$), need more water to refill the soil profile to become available for subsequent crops. Examining ΔS at different times and depths can inform growers of

where water us being used in the soil profile, the extent of a crops root zone, crop stage, and irrigation needs. In situ ΔS measurements can be combined with other measured WBCs or used with local WBC estimates from external databases to develop site specific water budget models.

A variety of approaches exist to measure ΔS, the most popular being direct soil core sampling, neutron probe moisture meters, time domain reflectometry (TDR) sensors, and frequency domain reflectometry sensors (FDR). ΔS can be easily calculated as the difference between volumetric water content (θ, cm^3/cm^3) (the ratio of volume of water to total volume of soil sample) at two points in time. If measurements of are available, θ can be calculated using *Eq 2*.

$$Eq\ 2\text{:}\quad \theta = \frac{V_W}{V_T} = \rho_b w$$

Where V_W (cm^3) is volume of water in a soil sample, V_T (cm^3) is the total volume of a soil sample, ρ_b is the soil bulk density (g/cm^3 cm^3), and w is the soil gravimetric water content (g/g).

Direct measurement of θ by soil core sampling is universally accepted as the most accurate and precise method (IAEA 2008). When performed correctly, this method is accurate to +/- 0.01 cm^3cm^{-3} (IAEA 2008). Soil cores are usually collected with a hand auger or a machine (i.e. geoprobe, giddlings probe) with a known volume. Samples are immediately weighed and then oven dried to calculate the volume of water present in the soil at the sampling date (θ). While effective, this method is labor intensive, does not capture ΔS fluctuations at small time steps (only between sampling dates), and does not allow for repetition of measurements in the exact same location.

The neutron probe moisture meter uses radioactive material to track the emission of neutrons. When neutrons collide with hydrogen, they lose energy and slow down. By tracking the density of these low energy neutrons, the neutron probe can provide a proxy for soil moisture (Devincentis 2020; IAEA 2008; Li et al. 2003). The advantages of the neutron probe are that once installed, soil moisture can be collected in the same location whenever needed and at desired depths. While measurements are restricted to sampling dates, the frequency of sampling can be significantly higher than taking manual sampling cores. It is, however, a very costly piece of equipment that comes with risk of working with radioactive material. There have also been reports of clay content and soil bulk density skewing neutron probe measurements (Li et al. 2003).

TDR sensors have become increasingly popular due to their ease of use and lower price compared to the neutron probe (Stangl et al. 2009; IAEA 2008). TDR sensors use the travel time of an electric pulse across a known length of metal transmission lines (wave guides) to calculate the dielectric permittivity, or degree of polarization, of a material being acted upon by an electric field (IAEA 2008; Ledieu et al. 1986; Kelleners et al. 2005). The permittivity of water is high, around 80 Fm^{-1}/Fm^{-1}, while the permittivity of air (1 Fm^{-1}/Fm^{-1}) and soil components (2-5 Fm^{-1}/Fm^{-1}) are quite low allowing for change in permittivity to be attributed to change in water volume (Topp et al. 1998; Ledieu et al. 1986). A direct empirical relationship between permittivity and θ allows the TDR sensor to report soil moisture to the user (Kelleners et al. 2005; Ledieu et al. 1986; Topp et al. 1998). TDR sensors are easy to install and can collect soil moisture measurements at a time step programmed by the operator, but they are limited to measuring soil moisture in smaller volumes of the surrounding soil compared to the neutron probe. Accurate readings are

dependent on good contact between the soil and the TDR sensor; air gaps will cause an underestimation in dry soil and over estimation of soil moisture in saturated soil (IAEA 2008; Stangl et al. 2009). While there have been reports of clay content disrupting TDR measurements, error in most soils is estimated as 0.02 m^3m^{-3} and calibration is usually only recommended in high clay content soils (IAEA 2008). Overall, TDR sensors provide an accurate, safe, nondestructive, portable, and easily automated way to estimate ΔS and will be the measurement technique focused on in this research, specifically a new multi-depth downhole TDR sensor (SoilVUE-10, Campbell Scientific) that measures to a depth of 1 m.

FDR sensors also use the dielectric properties of a material to determine θ. They consist of two metal rods inserted into the soil which together act as a capacitor. An oscillating current is sent through the soil between the rods and its frequency is logged by the sensor. The oscillation frequency can be related to a capacitance which is affected by the soil permittivity (IAEA 2008; Hardie 2020). Thus, small changes in water content will change the frequency output of the sensor. θ can be calculated from resulting permittivity values or through soil water and frequency count calibration curves. The main difference between FDR and TDR sensors is their sensitivity to soil texture, electrical conductivity, and temperature making them more prone to error. Similarly to TDR sensors, FDR sensors require careful installation and good contact with the soil to produce accurate readings (Hardie 2020; IAEA 2008).

Capturing ΔS in high clay content soils has proven to be difficult since clay physical properties may interfere with TDR measurements, however these interferences are reportedly less than the other technologies reviewed above (Abdullah et al. 2018; Stangl et al. 2009; IAEA 2008). One major source of error stems from the combination of bound and

free water in soils. Free water is able to move around soil pores, while bound water is attached to the soil surface by adhesive, cohesive, and osmotic bonds (Gong et al. 2003). Bound water is less polarized by an electric field than free water is, and thus can lower the permittivity of clay soils causing an underestimation of soil moisture by TDR sensors (Gong et al. 2003). Clay also impacts soil electrical conductivity. Clay colloid surfaces possess an electrical charge and increase the soils total electrical conductivity. In turn, permittivity increases, and TDR sensors are more likely to overestimate soil moisture (Kelleners et al. 2005; Gong et al. 2003). Due to this limitation, TDR sensors need site specific calibration if clay content is above a certain threshold recommended by the sensor manufacturer.

The shrink-swell capacity of clay soils can also affect TDR soil moisture measurements by causing soil separation from the sensor. In these cases, data must be discarded or extrapolated. Clay soils swell as soil moisture increases and shrink as soil moisture decreases due to the capacity of clay minerals to absorb water, therefore percent clay content directly influences soil shrink-swell potential (Chertkov 2012; Gomboš et al. 2012). Shrink-swell behaviors of clay soil as a response to natural wetting and drying cycles has been well documented and soil moisture as a function of shrink-swell potential is well known (Grossman et al. 2002; Gomboš et al. 2012; Widomski et al. 2015; Malongweni et al. 2019; Chertkov 2012). The degree of shrink-swell potential is quantified by the coefficient of linear extensibility (COLE), or the percent volume change of a wet soil (often water content at 1/3 bar (field capacity)) to a dry soil (often oven dryness) (Gomboš et al. 2012; Widomski et al. 2015). Changes in porosity and bulk density across different soil moistures can also be used to assess shrink-swell potential (Chertkov 2012; Malongweni et al. 2019; Grossman et al. 2002). The shrink-swell potential of soils is dependent on percent

clay content, more clayey soils will have a higher shrink-swell potential or greater COLE values (Hashim et al. 2006; Gomboš et al. 2012). When clay shrinks, the soil may form macropores (or large cracks) causing soil separation and sensor exposure to the atmospheres. When this occurs, TDR sensors may overestimate soil moisture in wet conditions as free water collects in the macropore in direct contact with the sensors. Likewise, exposed TDR sensors may underestimate soil moisture in dry conditions since the atmosphere has less soil moisture than soil. Site-specific calibration is recommended for TDR sensors to account for sensitivity to clay content and improve accuracy (IAEA 2008; Stangl et al. 2009; Gong et al. 2003; Kelleners et al. 2005).

The goal of this research was to develop field scale soil water budgets in agricultural systems with clayey soils using a new type of TDR sensor (TDR sensor-10, Campbell Scientific). The TDR sensor being used is a fairly new instrument with limited to no publications. We look at winter-cropped rice fields in the Sacramento Valley, CA as a case study. Rice is grown in soils characterized by high clay content to reduce water loss and retain water level when rice is flooded. The case study evaluates the hydrologic impacts of winter crops in rice systems during the non-rice growing season. We performed instantaneous and continuous soil sampling and soil texture analysis to show the relationship between clay content and TDR sensor performance. ETc was estimated as the residual of the water budget and WBCs were analyzed at daily and seasonal time steps to track water distributions. We report difficulties encountered when using the TDR sensor, calibration methods, and compatibility with water budget modelling. Findings from this research will be used to improve experimental design and methods in future years of this study and provide recommendations for TDR sensor users.

California Context

California faces unique water management challenges that are exacerbated by changing climate and increasing population, propagating the uncertainty of water supply for the country's leading agricultural state in farm-level sales (Johnson et al. 2015) . Recent droughts and aging water resources infrastructure have highlighted the imminent danger to human and environmental health as the state's water demand continues to grow (Douville et al. 2021). CA agriculture consumes 40% of total water use, 80% of human allocated water use, and 3.2 million irrigated farm hectares (Mount et al. 2019; Johnson et al. 2015). The current level of water consumption cannot be maintained if production levels continue, and more sustainable agricultural water management must be considered in grower decision making (Devincentis 2020). Additionally, alteration of quality, quantity, and timing of water supply has disrupted natural ecological functions such as fish spawning habitat, streamflow to support flora and fauna, sediment transport, and nesting grounds for migratory birds (Bunn et al. 2002). Agroecology is a holistic, interdisciplinary approach that focuses on optimizing interactions and outcomes for humans, flora, fauna, and the physical environmental in agricultural systems. The potential of agroecosystems as a tool to increase agricultural water management sustainability, efficiency, and ecosystem resilience has been recognized and requires more system specific technical knowledge and water budget information (Devincentis 2020; La Hue, n.d.; Johnson et al. 2015).

This research aims to better understanding the intersection of agroecosystems and water management in Sacramento Valley rice systems. California is the second largest producer of rice in the United States with 95% of production concentrated in the

Sacramento Valley (Linquist et al. 2015; Strum et al. 2013). Historically, the Sacramento Valley was covered in seasonal wetlands which provided habitat for resident and migratory birds on the Pacific Flyway (Frayer et al. 1989). Now more than 90% of wetland areas have been lost or transformed to agricultural fields, predominantly rice (Strum et al. 2013; Frayer et al. 1989). However, winter management practices such as flooding and cropping during the non-rice growing season have provided alternative habitat for bird populations (Strum et al. 2013).

While flooding is not a viable option during drought years, planting winter crops provides sufficient vegetative cover for bird habitat, yet their effects on field scale water budgets are understudied and may be preventative to higher adoption (Strum et al. 2013; Pettygrove et al. 1996). In a normal rice cropping schedule, winter crops are planted after rice harvest, gown from November to early April, and rice is planted again in May (*Table 1*). However, field management for spring termination of winter crops and prep for rice planting occur during the critical nesting period for many resident and migratory birds (April-July), often destroying nests and eggs (Central Valley Bird Club 2017; LaRose et al. 2018; Lokemoen et al. 1997). Rice fields that will be fallowed (instead of planted with rice) have the unique opportunity to provide nesting habitat birds by extending the growing period of winter crops and shifting termination from April to mid-July.

Some rice fallowing is related to organic production, but rice fallowing for the purpose of water sales and transfers has increased due to the state's complicated water challenges and increased drought that have put pressure on rice growers (Hanak et al. 2019). The USDA 2021/2022 Rice Outlook indicated 190,607 hectares of planted rice in California, a 9% decrease from the previous year due to water shortages (Childs 2021).

These water sales are based on the amount of water that would have been consumed by the rice crop (889-1,143 mm) during that irrigation season, equivalent to the crops ETc (California Department of Water Resources and Bureau of Reclamation 2019; California State Water Resources Control Board 1999; Wong et al. 2021; Lal et al. 2012). Developing a better understanding water budgets during dry years when rice growers are asked to fallow their fields could aid conservation strategies in offering ecological benefits for birds and water for sale/transfer (Linquist et al. 2015; Strum et al. 2013).

This study considers extending the winter crop growing season during fallow years to provide critical bird nesting habitat (*Table 1*). This action would most likely be adopted by rice growers provided winter crops consume significantly less water (have a smaller ETc) than rice and have an ETc closer to that of fallowed land. Under these circumstances, the difference between winter crop ETc and rice ETc is still available for sale/transfer. Currently, there is a lack of research on hydrologic processes in winter cropped rice systems, specifically during nesting periods, to guide growers in these decisions. We examine patterns in WBCs in winter cropped and in fallowed rice systems using field scale water budgets and examine the success of TDR sensors in the clayey soils characteristic of these systems.

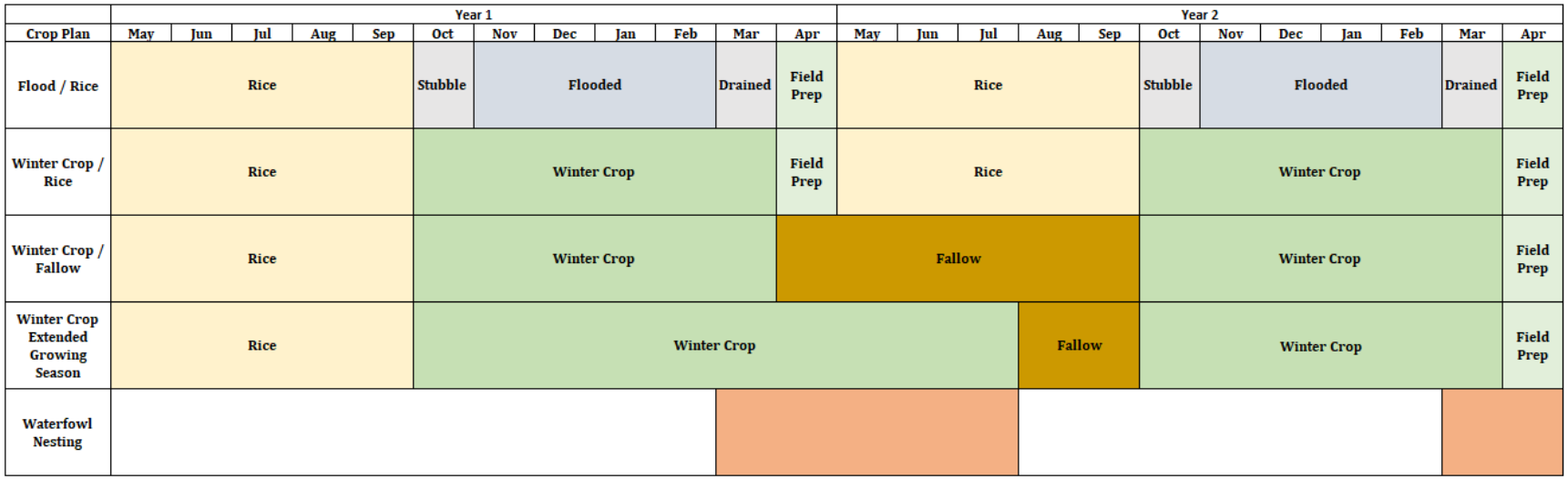

Table 1: Possible 2-year cropping schedules for rice systems in the Sacramento Valley. Calendar begins at the start of the rice growing season.

Methods

The overall goal of this study was to develop field scale water budgets in winter-cropped rice systems and evaluate multi depth down-hole TDR sensors in clay soils over the period of winter crop growth. We accomplished our goal by quantifying the hydrologic impacts of three treatments in post-harvest rice systems during the non-rice growing season: (1) fallow; (2) winter-cropped with non-irrigated vetch; (3) winter-cropped with irrigated winter wheat. Emphasis was placed on the determination of ΔS through continuous soil moisture measurements and instantaneous soil core sampling, the effect of soil clay content on soil sensor monitoring, and water budget analysis to understand seasonal distribution of water inflows and outflows. Soil moisture, water table height, ETc, and runoff were monitored in-situ at each site while precipitation and irrigation were obtained from external sources. One central data logger (CR3000 data logger, Campbell Scientific) was installed at each field and powered by solar panels to collect soil moisture and water table height data. Surface runoff was measured at each field's lowest point of elevation where the fields drain using weirs, water level loggers, and digital cameras. Datasets were then analyzed to compare cumulative changes in WBCs, seasonal distributions of water use and loss, water budget closure, and the accuracy of TDR sensors at each site (*Fig 1*).

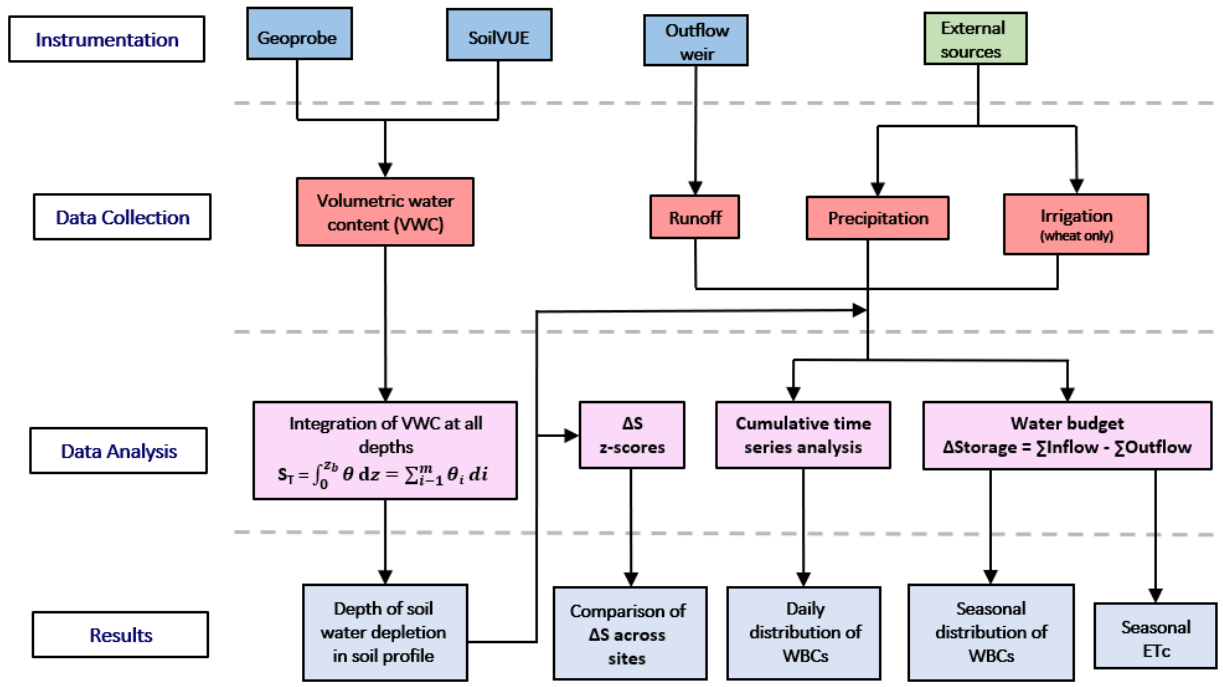

Fig 1: Project workflow.

Site and Soil Description

This study was located in the Sacramento Valley, the main rice growing region of California. Vetch and winter wheat sites were on farms located within 2.5 km of each other in Sutter County, while the fallow site was 72.4 km north in Butte County at the Rice Experiment Station (*Fig 2*). The planned hydrologic period of study is 6 years with this analysis occurring in year 2, examining the first full year of data (year 2). Monitoring took place Nov. 2020 – July 2021 with each site hosting one of the three treatments. Exact dates of monitoring were adjusted for field specific agronomic management requirements to enable smooth field operations and maintain grower relationships (*Table 1*). All sites were planted with rice during the previous growing season and winter crops were seeded just prior to the start of monitoring. Sites differ in historical cropping patterns, management practices, precipitation patterns, and average temperature.

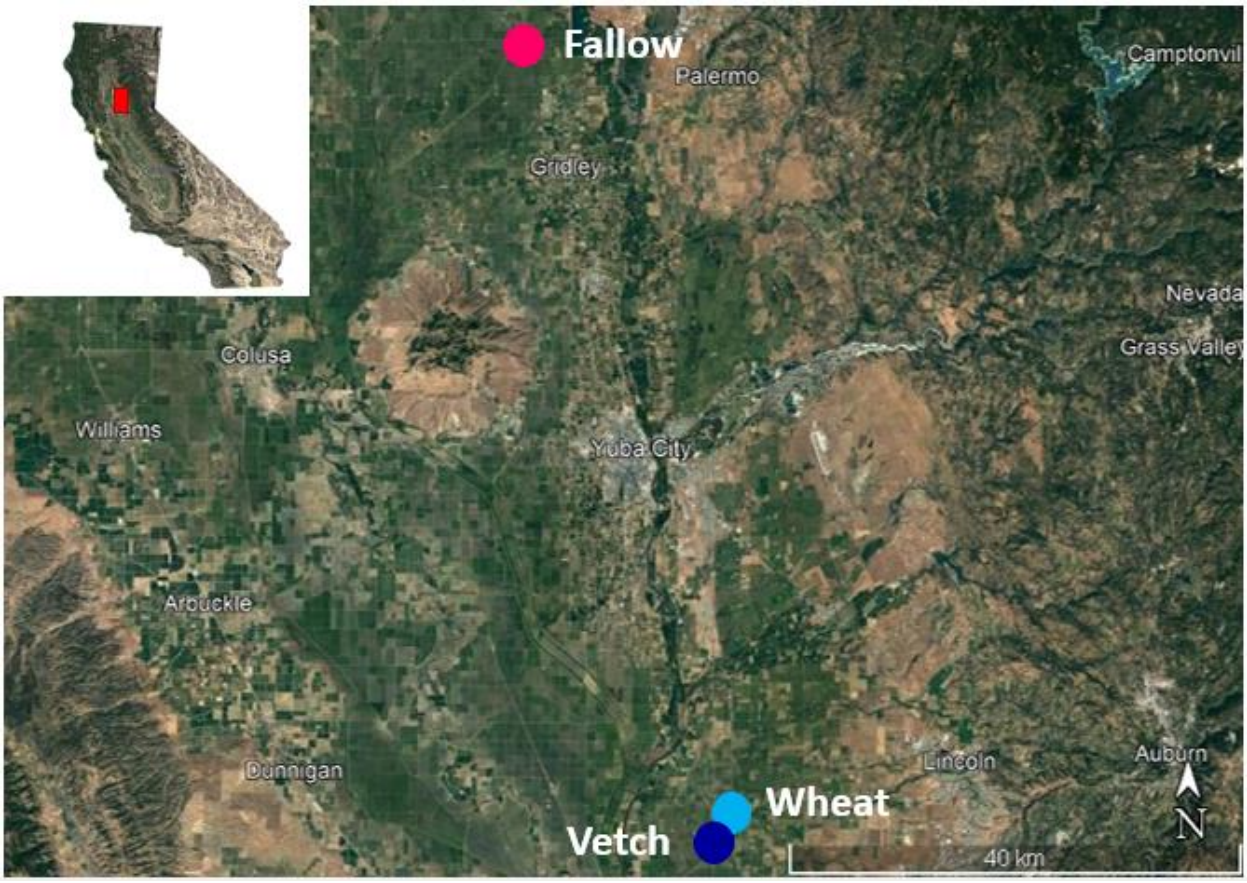

Fig 2: Site map.

The NRCS soil survey classifies soil at the vetch site as approximately 50% poorly drained Clear Lake clay (Fine, smectitic, thermic Xeric Endoaquerts) and 50% moderately well drained Marcum clay loam (Fine, montmorillonitic, thermic Typic Argixerolls. The winter wheat site consisted of predominantly poorly drained Clear Lake silt loam (Fine, montmorillonitic, thermic Typic Pelloxererts) and smaller amounts (<10%) of Marcum clay loam. Soils at the fallow site are classified as poorly drained Esquon-Neerdobe clay (Fine, smectitic, thermic Xeric Epiaquerts; Fine, smectitic, thermic Xeric Duraquerts) (NRCS 2021). Additional soil characteristics were collected from the NRCS Soil Web Survey (*Table 3*).

	Soil Cores			TDR sensor, ETc, water table, runoff	
	start 2020	mid 2021	end 2021	start 2020	end 2021
Fallow	11/14	3/5	6/29	11/14	6/29
Vetch	11/14	3/4	7/21	11/14	7/15
Winter wheat	11/14	3/4	7/1	11/12	6/14

Table 2: Field monitoring calendar.

Soil Type	Site	Linear Extensibility (%)	Field Capacity (θ at ⅓ bar)	Permanent Wilting Point (θ at 15 bar)	Depth to Water Table (cm)	Bulk Density at field capacity (g/cm^3)	Depth to restrictive layer (cm)
Clear Lake Silt Loam	Winter wheat	5.2	0.360	0.218	122	1.38	>200
Marcum Clay Loam	Winter wheat; Vetch	6.5	0.364	0.257	>200	1.45	>200
Clear Lake Clay	Vetch	12.3	0.420	0.324	25	1.32	>200
Esquon-Neerdobe	Fallow	9.1	0.286	0.163	76	1.39	142

Table 3: Soil physical properties obtained from the NRCS Soil Web Survey.

Data Collection

Soil Moisture

Instantaneous data

Soil core samples were taken at the beginning, middle, and end of the monitoring season to assess changes in soil properties and calculate seasonal ΔS. Start and end of season soil cores were taken within a week of planting/harvest with a Geoprobe drilling rig down to a depth of 2.4 m. Because driving the Geoprobe onto fields would greatly disturb established winter crops, mid-season soil cores were collected manually with a 3.81 cm

diameter hand auger to a depth of 0.9 m. Samples were collected at four sampling locations per site, 1 sample per 0.3 m of soil depth, for a total 201 samples over the course of the season (*Fig 3*). Sampling locations were determined using a lose structured zone based sampling to capture different geographic areas of the field, where sample 4 was always taken near the data logger. We assumed minimal to no drainage past the depth of our observation (2.4 m) on the fallow field since the soil is estimated to have a restrictive duripan layer at 0.5-1.0 m (NRCS 2021). Drainage past the depth of our observation was plausible on the vetch and winter wheat fields since restrictive layers are estimated at more than 2.0 m (NRCS 2021).

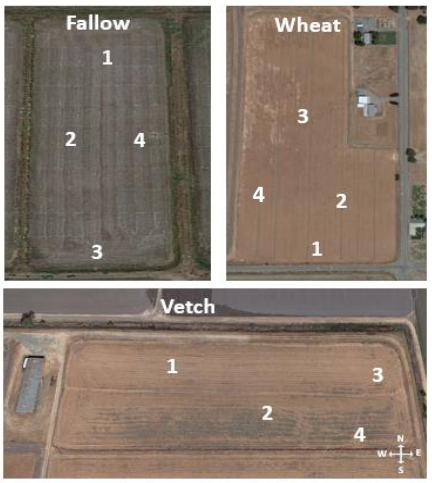

Fig 3: Soil core sampling map

Start of season and end of season sample wet weights were measured in the laboratory within 2 days of data collection. Samples were dried at 105°C for a minimum of 120 hours due to the high clay content of the soil. Gravimetric water content (w, g/g), which describes the ratio of the mass of water to mass of solids, was calculated using the wet weight (M_w, g) and dry weight (M_d, g) of each sample (*Eq 3*).

$$\textit{Eq 3:}\ \mathrm{w} = \frac{M_{w-} M_s}{M_s}$$

Bulk density (ρ_b, g/cm^3) was calculated using M_d and the total volume (V_T, cm^3) of each sample (*Eq 4*) and was used to check for potential compaction at sampling locations.

$$Eq\ 4:\ \rho_b = \frac{M_s}{V_T}$$

Porosity (n, g/cm^3 / g/cm^3) was estimated using ρ_b and a generally accepted particle density (ρ_s, g/cm^3) for minerals of 2.65 g/cm^3 (*Eq 5*)(Blake 2008). The difference in ρ_b and n between mid-season (representation of wet season soil conditions) and end of season (representation of dry season soil conditions) soil cores were to evaluate changes in soil structure from shrinking/swelling. Coefficients of linear extensibility (COLE) were calculated using *Eq 6* to provide further support of shrink-swell potential in soils. Calculated COLE values were then compared to shrink-swell potential soil classification (*Table 4*).

$$Eq\ 5:\ n = 1 - \frac{\rho_b}{\rho_s}$$

$$Eq\ 6:\ COLE = \left(\frac{\rho_{bDry}}{\rho_{bWet}}\right)^{(1/3)} - 1$$

Shrink-swell potential	**COLE**
Low	<0.03
Medium	0.03-0.06
High	0.06-0.09
Very High	>0.09

Table 4: Shrink-swell potential by COLE for soils (Parker et al. 1977).

Volumetric water content (θ, cm^3/cm^3) which describes the ratio of water volume (V_W, cm^3/cm^3) to total volume of the sample (V_T, cm^3/cm^3) was calculated for start and end of season soil cores using ρ_b and w (*Eq 2*). All θ calculations used end of season bulk density values since both samples were collected during the dry season with minimal clay swelling.

The depth of water in each soil layer (S, mm) was calculated using the θ and thickness of the soil layer (d, mm) (*Eq 7*). The total depth of water in the vertical soil

profile (S_T, mm) was found by integrating θ values across all soil layers according to *Eq 8* (Zhao et al. 2020).

$$Eq\ 7\text{: } S = \theta d$$

$$Eq\ 8\text{: } S_T = \int_0^{Z_b} \theta\, dz = \sum_{i=1}^{n} \theta_i\, d_i$$

Where Z_b (mm) is the maximum computational soil profile depth, θ_i ($cm^3/cm3$) is the θ of layer i, d_i (mm) is the thickness of layer i, and n is the number of calculation layers. Change in soil water storage (ΔS, mm) over a given time period was calculated by *Eq 9*.

$$Eq\ 9\text{: } \Delta S = S_2 - S_1$$

Where S_2 (mm) is the depth of soil water at time 2 (i.e., end of the measurement season) and S_1 (mm) is the depth of soil water at time 1 (start of the measurement season).

To assess site specific soil textures, start of season soil samples were sent into the UC Davis analytical laboratory for particle analysis. Average percent silt, sand, clay at each depth across were calculated across sampling locations for each site.

Continuous data

Daily changes in θ were measured to a depth of 1m using a multi depth down-hole TDR soil moisture and temperature profile sensor (SoilVUE-10, Campbell Scientific). One sensor per site was installed at each data logger location in mid-November 2020 removed within one week of harvest to accommodate field management activities (*Table 2*). Sensors were installed by first drilling an installation hole using a Geoprobe drilling rig and then screwing the sensor into the ground so that good contact between the sensor and soil was established. The TDR sensor measures θ, permittivity, electrical conductivity, and

temperature at multiple depths (5, 10, 20, 30, 40, 50, 60, 75, and 100 cm) using time domain reflectometry (TDR) technology.

The TDR sensor requires site specific calibrations for soils >45% clay. Percent clay content from soil core particle analysis was used to determine the necessity of calibration with 0-0.3 m cores compared to 5, 10, 20, 30 cm, 0.3-0.6 m cores compared to 40, 50, 60 cm, and 0.6-0.9 m cores compared to 75 and 100 cm TDR sensor depths. The winter wheat TDR sensor did not need calibration since no soil samples were identified with >45% clay. Both the fallow and vetch TDR sensors did require site specific calibration since soil samples were identified with >45% clay. Each TDR sensor was submerged in a 44-gallon plastic container full of site-specific soil thoroughly mixed with water. The TDR sensor was programmed to collect data at 1 min intervals for 30 min. During data collection, soil subsamples were collected at each sensor depth using a 13.7 cm diameter round stainless-steel cutter to determine the true θ. Subsamples were weighed immediately, oven dried at 105°C for a minimum of 120 hours, and θ was calculated using *Eq 2*. This process was repeated for 4 different soil saturation levels and is the recommended site-specific calibration procedure outlined from the sensor manufacturer, Campbell Scientific (Baker et al. 2021). This process was laborious and only partially effective for multiple reasons. First, site specific soil for the calibration process was collected at the end of the season in July. The recent extreme temperatures and lack of precipitation resulted in dry, constricted soils that were impossible to penetrate past a depth of 0.6 m, hence the heterogeneity of the entire soil profile monitored by the TDR sensor was not obtained or represented in the calibration process. The quantity of soil required to submerge the TDR sensor was large. Collected soil had formed large, solid aggregates when drying over spring and had to be

ground down by hand which was time consuming and required large amounts of physical labor. When saturating the soil, it was difficult to form a homogeneous mixture. Once water was applied, the dry soil immediately began to form aggregates of both dry and moist soil. After multiple attempts we obtained a mixture that was acceptable to the best of our ability, but restricted sample size, saturation range, and soil profile representation likely impaired the results.

Based on the relationship described in Ledieu et al. (1986), true θ was compared to TDR sensor permittivity readings to develop calibration curves for each sensor depth using linear regression (Appendix 1). Calibration curves were applied to raw data, only at depths with >45% clay. Calibrated data was visually inspected and compared to uncalibrated data to evaluate the improvement with calibration. The fallow TDR sensor was calibrated at depths of 5 and 10 cm only and the vetch TDR sensor at all depths. The 100 cm sensor depth of the Vetch TDR sensor was found to need maintenance by Campbell Scientific and was removed from data processing. S, $S_{T,}$ and ΔS were calculated using calibrated data and *Eq* 7, 8, and 9.

Beginning in mid-May 2021 the fallow TDR sensor recorded high amounts of noise; θ for this time period was estimated using linear and exponential regressions to find best fit trend lines at each sensor depth. The 75 cm sensor depth of the Vetch TDR sensor recorded faulty θ values beginning in mid-May with no system inputs and was estimated using linear interpolation for the remainder of the season. Additional gaps in data were estimated using linear interpolation for small gaps and a mix of linear, exponential, and logarithmic regressions to find best fit trend lines at individual sensor depths.

Water Table

Pressure transducers (Acculevel by Keller America) were installed near TDR sensors by drilling a hole with the Geoprobe, inserting perforated PVC into the hole, and lowering the pressure transducer to the depth of the TDR sensor and expected rootzone. The pressure transducer was connected to the main datalogger for continuous data collection and measured changes in the height of the water table and served as a verification of TDR sensor readings when the height was between the surface and the depth of the TDR sensor (1m).

Runoff

Rectangular weirs combined with water level data loggers (Global Water-WL16) were installed at the lowest points of elevation in each field to quantify runoff. Discharge drains were fitted for custom weirs at the fallow and vetch fields; the winter wheat field was surveyed, and a weir was constructed at the perimeter's lowest point. Data loggers were attached to wooden stakes and placed within 0.6 m of the weir outlet and took daily measurements of the height of water flowing over the weir; stadia rods were placed directly behind the data loggers. Daily photos were taken on wildlife cameras that were placed in front of the data loggers, facing the weir, to verify data logger readings with stadia rod readings.

Water height and camera data from all sites were evaluated and considered negligible since water never reached the height of the weir opening, and camera footage showed minimal to no ponding in front of the weirs.

Precipitation and Irrigation

Daily precipitation data was collected from the California Irrigation Management Information Systems (CIMIS) database, a widely used weather data network run by the California Department of Water Resources (CIMIS 2021). CIMIS manages a large network of weather stations randomly distributed throughout California with the goal of assisting irrigators with water management. The closest stations to our fields were selected, and precipitation data was downloaded for the monitoring period. The winter wheat field was irrigated while the vetch was not. Irrigation estimates were given to us by the grower and validated through differences in soil moisture for the identified irrigation period.

Data Analysis

Soil Analysis

All data analysis was done in Microsoft Excel Version 2110 and R 4.1.0. Soil spatial heterogeneity was evaluated by analyzing soil physical characteristics and calculated ΔS values across sampling locations and depths. Particle analysis results from the start of season soil cores were analyzed by developing linear regression models to assess percent clay as a function of depth.

Changes in ΔS were evaluated at a seasonal and daily timestep. Geoprobe soil cores were used to calculate seasonal ΔS since they covered a larger depth of 2.4 m, while the TDR sensor only covered 1 m. The TDR sensor data was used estimate averaged, daily ΔS and obtain higher resolution of temporal and spatial (per depth) soil moisture dynamics. Continuous ΔS estimates from the TDR sensor provided insight into changes of soil moisture at depths of the soil profile during different phases of winter crop growth. Fractional soil moisture was calculated by identifying the point of maximum volumetric

water content over the course of the season and dividing all subsequent daily TDR sensor readings by this value. Fractional soil moisture provides a method for comparing heterogeneous data sets by normalizing data from different sites to one scale (Devincentis 2020). Soil moisture data from all sites could then be compared on the same scale to see the percentage of peak soil moisture retained by each site at the end of the season. This method was especially applicable given that precipitation patterns were similar across all sites.

Another way to compare data sets from different distributions and ranges is by scaling data to fit within a 0-1 range using z-score standardization. Z-scores transform each data set so that the mean (μ) is 0 and the standard deviation (σ) is 1 (*Eq 10*).

$$Eq\ 10:\ z = \frac{x - \mu}{\sigma}$$

Where z is a new, scaled datapoint. Positive z values indicate the raw data point is above the temporal mean and negative when below (cite standardized time series). Because z-scores are centered around the same value (0), all sites can be compared to understand performance relative to each other. Daily TDR sensor z-score data and new distributions were generated to observe temporal changes in S.

Water Budgets

Monitored WBCs (P and ΔS) were analyzed at a daily time step to see trends over time. Cumulative plots of averaged, daily WBCs were used to compare the observed magnitude of TDR sensor ΔS to precipitation inputs as a means of evaluating TDR sensor accuracy at a daily time step.

Water budget models were developed at a seasonal time step to understand distributions of water use and loss over the extended winter crop growing season.

Seasonal ETc was calculated as the residual of the water budget where our measurements showed that *RO* was close to zero and *D* as assumed negligible (*Eq 11*).

$$Eq\ 11:\ ETc = P+I - \Delta S - RO$$

Seasonal water budgets using soil core versus TDR sensor were compared to evaluate TDR sensor accuracy at a seasonal time step.

Results and Discussion

Soil Characteristics and Drivers

Clay content was of particular interest in this study because of its prevalence in rice systems and difficulty in obtaining accurate soil water measurements. By examining the entire 2.4 m soil profile, we found statistically significant relationships between percent clay and soil depth in the fallow (R^2=.0.7131, p=3.077e-08) and vetch (R^2=0.8581, p=4.248e-12) sites, while no relationship was found in the winter wheat field (R^2=0.03255, p=0.4101) (*Fig 4*). At both the fallow and vetch sites, more clay is found near the soil surface and clay content decreases as depth increases. The winter wheat soil profile is dominated by sand below a depth of 0.3 m (44-59% sand depending on depth). A complete description of soil texture (% clay, sand, and silt) by depth is shown in *Fig 5* and can be found in Appendix 2.

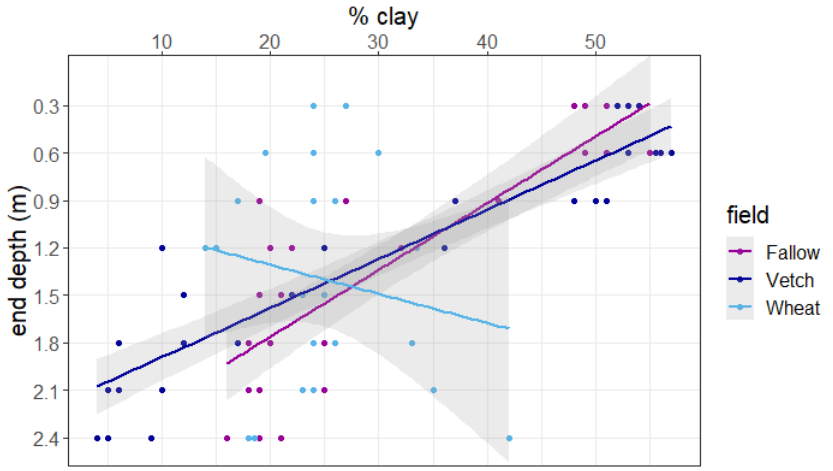

Fig 4: Linear regression model of percent clay content and depth of soil profile for all sites.

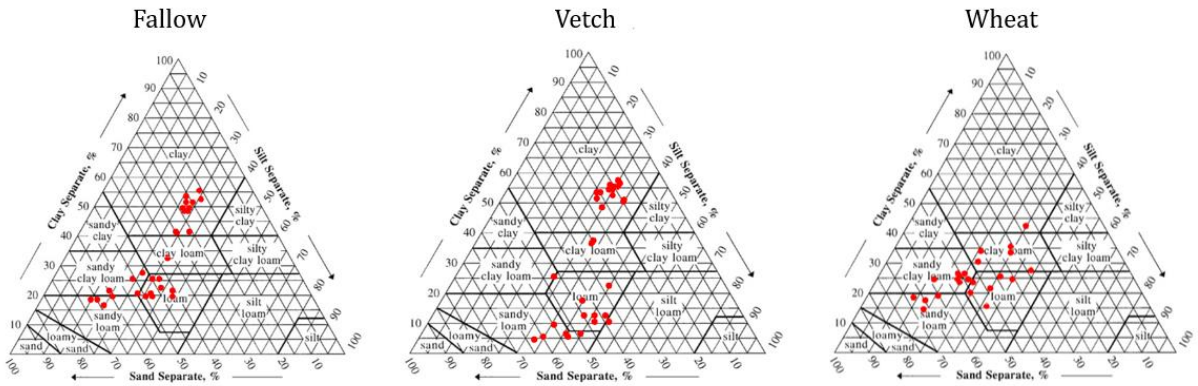

Fig 5: USDA soil textural classification for 0.3 m soil samples taken to a 2.4 m depth at all sampling locations at each site.

To observe the magnitude of soil shrink-swell potential, changes in average bulk density (ρ_b) and porosity (n) during the dry and wet season were estimated using mid-season soil cores, where soil was more saturated, and end of season cores, where soil was dry (*Table 5*, Appendix 3). Estimates were for the first 0.9 m of the soil profile where all heavy clay soils (>45%) exist. At all sites we observed an increase in ρ_b and decrease in *n* from mid-season to end of season confirming the existence of shrink-swell potential. Fallow had an average change in bulk density of $\Delta\rho_b$=0.43 and change in porosity Δn=-0.17;

vetch had an average $\Delta\rho_b$=0.32 and Δn=-0.12; and winter wheat had an average $\Delta\rho_b$=0.38 and Δn=-0.15. Increases in ρ_b and decreases in *n* during the course of the season suggest that total soil volume is significantly larger when soils are more saturated and shrinks as soils dry.

These findings align with the literature and are further corroborated by the calculated coefficient of linear extensibility (COLE) (*Table 4)*. When compared to the accepted soil shrink-swell potential classification, calculated COLE values at all sites align with soils that posses "very high" shrink-swell potentials (>0.09). COLE calculations here are representative of soil volume change from mid-season (wet soil) to end of season (dry soil) θ, as opposed to the more traditional calculation that uses field capacity (wet soil) and oven dry (dry soil) θ. Calculated COLE values are an indication of a possible source of the difficulties of we encountered when monitoring high clay content soils at our sites such as underestimation of θ from soil/sensor separation.

	mid-season θ (cm^3/ cm^3)	end of season θ (cm^3/ cm^3)	$\Delta\rho_b$ (g/cm^3)	Δn (cm^3/ cm^3)	COLE
Fallow	0.42	0.26	0.43	-0.17	0.12
Vetch	0.42	0.21	0.32	-0.12	0.09
Wheat	0.23	0.13	0.38	-0.15	0.10

Table 5: Average volumetric water content (θ) during mid-season and end of season soil core sampling dates.

There was high spatial variability of seasonal ΔS from soil cores across sampling locations. ΔS in the total vertical soil profile was both positive and negative in the fallow and winter wheat sites, while the vetch site was consistently negative (*Fig 5*). Positive ΔS values signify a net gain in soil water while negative values a net loss. These results show high heterogeneity within field sites and suggest that a greater number of soil samples per field could better capture average ΔS.

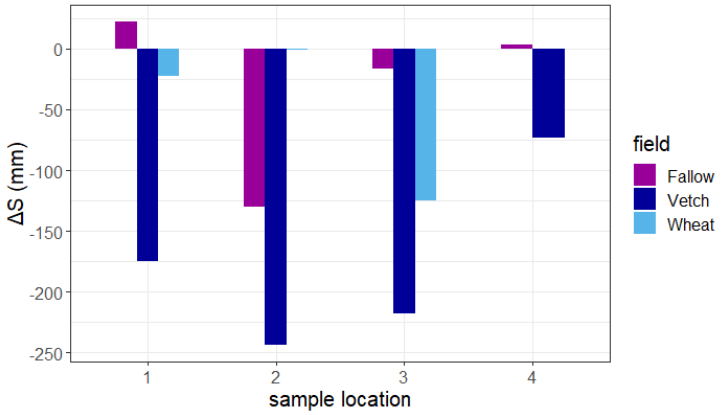

Fig 5: Seasonal change in soil moisture (*ΔS*) for total vertical soil profile across sampling locations.

Average seasonal *ΔS* by depth (0-2.4 m) was analyzed. The fallow site experienced a decrease in *ΔS* throughout the soil profile, except for at 8ft (*Fig 6*). High clay content and biomass residual left over from the previous season may have reduced evaporation from the soil surface and lateral flow from surrounding fields could have increased *ΔS* at lower depths. The vetch site had a seasonal loss of soil moisture (*-ΔS*) at all depths, with significant decrease in the top 0.9 m surrounding the root zone. The winter wheat site had average decrease in *ΔS* in the top 1.5 m with most significant losses at the soil surface, however there were increases in *ΔS* at lower depths.

When examining θ by depth measured from the TDR sensor, inefficient irrigation application may have been a source of increase ΔS at lower depths of the soil profile. During the time of application, irrigation resulted in an increase in ΔS at all soil depths but more dramatically at depths closer to the soil surface (*Fig* 7). The winter wheat crop used soil water from the top layers of the soil profile first and pulled from lower depths as needed after irrigation (*Fig 7*). The large quantity of applied irrigation combined with sandier soil with higher hydraulic conductivity, resulted in infiltration of irrigation water past the TDR sensor measurement depth. Irrigation water at low depths was likely not used by the winter wheat crop, which has a maximum observed root zone to a depth of 2 m, causing a seasonal increase in ΔS with depth in the soi profile (Thorup-kristensen et al. 2009).

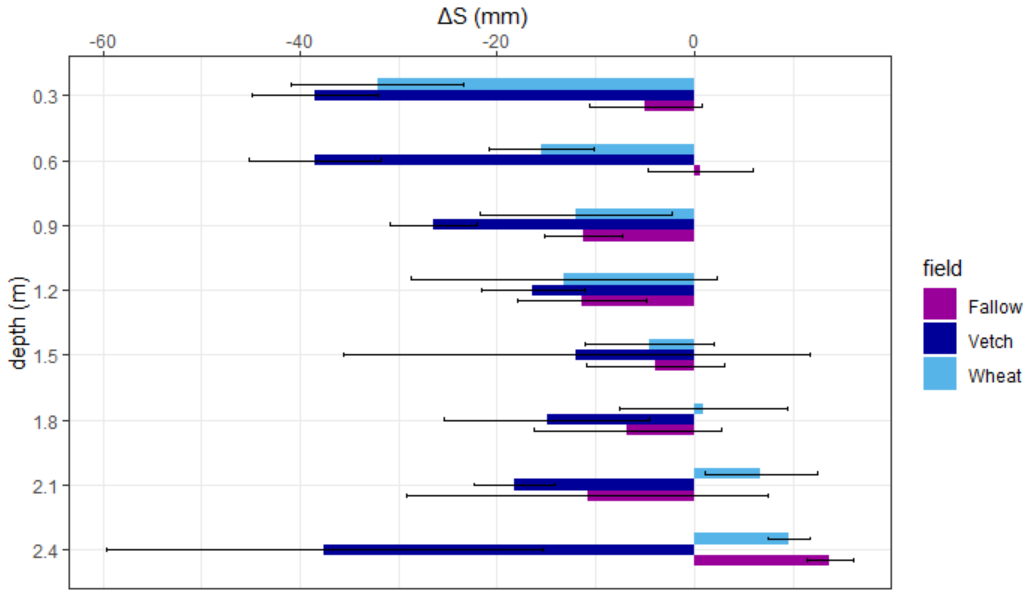

Fig 6: Average ΔS per depth of vertical soil profile with error bars of one standard error.

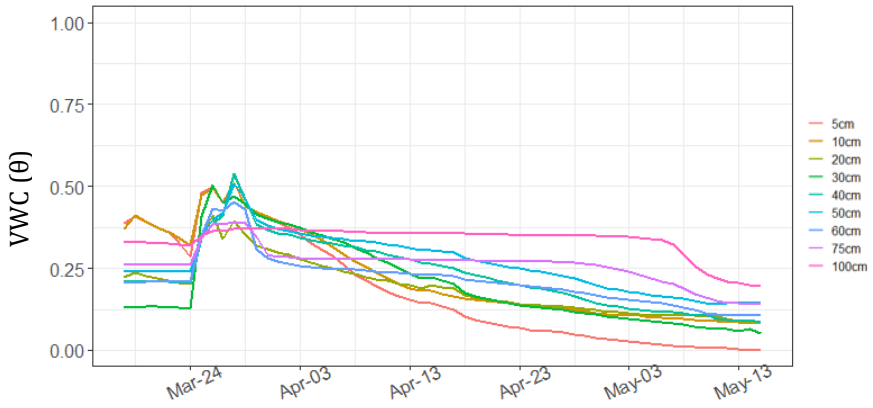

Fig 7: Volumetric water content (VWC, θ) by depth for winter wheat irrigation event.

Averaged daily TDR sensor data was analyzed to see θ trends over time. θ by depth for three precipitation events occurring on 12/11 – 12/18/20, 1/22-2/4/21, and 3/18/21 were plotted to evaluate wetting and drying patterns in the soil profile (*Fig 8*). These events were chosen because they occurred before the wheat's irrigation and were a good representation of seasonality (start, middle, and end). Together, these events made up 58% of seasonal precipitation that occurred at all sites (90.0 mm at fallow; 85.3 mm at vetch and wheat). At the fallow site, during the first large precipitation event of the season (12/11 – 12/18/20) water began to fill the upper soil layers while simultaneously infiltrating to lower depths. Once lower soil layers were saturated, the top 20 cm of soil experienced rapid, high magnitude, spikes in θ during the 1/22-2/4/21, and 3/18/21 events. Upper layers dried from evaporation and lower layers remained saturated once filled. Lower soil layers (40, 50, 60, 75, and 100 cm) saw little change in θ (0.47-0.56 cm^3/cm^3) and remained stable for most of the winter (Dec-April). θ at saturation for the lowest depths were confirmed by average mid-season *n* calculations estimated from soil

cores, which ranged from 0.54-0.64 (Appendix 3). n can be roughly equivalated to θ at saturation since it's the space water could occupy if all soil voids were filled.

The vetch experienced similar patterns to the fallow with the exception that the lowest depth (2.1 m) had lower θ than many intermediate layers. This may have been due to high clay content in the upper soil layers retaining soil moisture, preventing infiltration to lower depths. Mid-season n of vetch indicated a θ at saturation ranging from 0.56-0.63 cm^3/cm^3 (Appendix 3), which matches TDR sensor values in lower layers during the 12/18/20 event (*Fig 8*). θ begun to show a general decreasing trend during the 1/22-2/4/2, possibly due to the crop consuming water in the upper and middle soil layers.

Patterns in the winter wheat soil profile are more difficult to discern. Mid-season n of winter wheat indicates potential saturation at θ ranging from 0.47-0.59 cm^3/cm^3 (Appendix 3), which matches saturation ranges from the TDR sensor during all three events. The largest increases in θ magnitude occurred in the first 0.1 m of the soil profile during all events. However, increases in θ at the winter wheat site were significantly smaller than at the vetch and fallow, possibly due to lower clay and higher sand content promoting infiltration laterally or to lower depths, or due to the TDR sensor overestimating θ in high clay soils of the fallow and vetch. Intermediate soil layers in both the fallow and vetch retained a θ of approximately 0.5 cm^3/cm^3 when saturated, while the winter wheat was approximately 0.25 cm^3/cm^3. Again, this could be a result of clay soil's capacity to retain more water than sandier soils.

Distributions and time series were compared for TDR sensor raw, daily data and z-scores (*Fig* 9, *Fig 10*). Z-scores better distinguished differences in ΔS between sites. Most noticeable is the magnitude of ΔS during winter wheat irrigation. The raw data equates

winter wheat's seasonal max ΔS to vetch's seasonal max ΔS. While this is true, the z-score data provides more context in conceptualizing the magnitude of ΔS in response to winter wheat's irrigation event (max ΔS 3.38 standard deviations) compared to the rest of the season, and to the other sites (fallow max ΔS=1.79 standard deviations, vetch max ΔS =1.52 standard deviations). As temperatures rose without precipitation during the spring, fallow and vetch ΔS continue to deplete while winter wheat's soil profile is refilled from the irrigation event in late March.

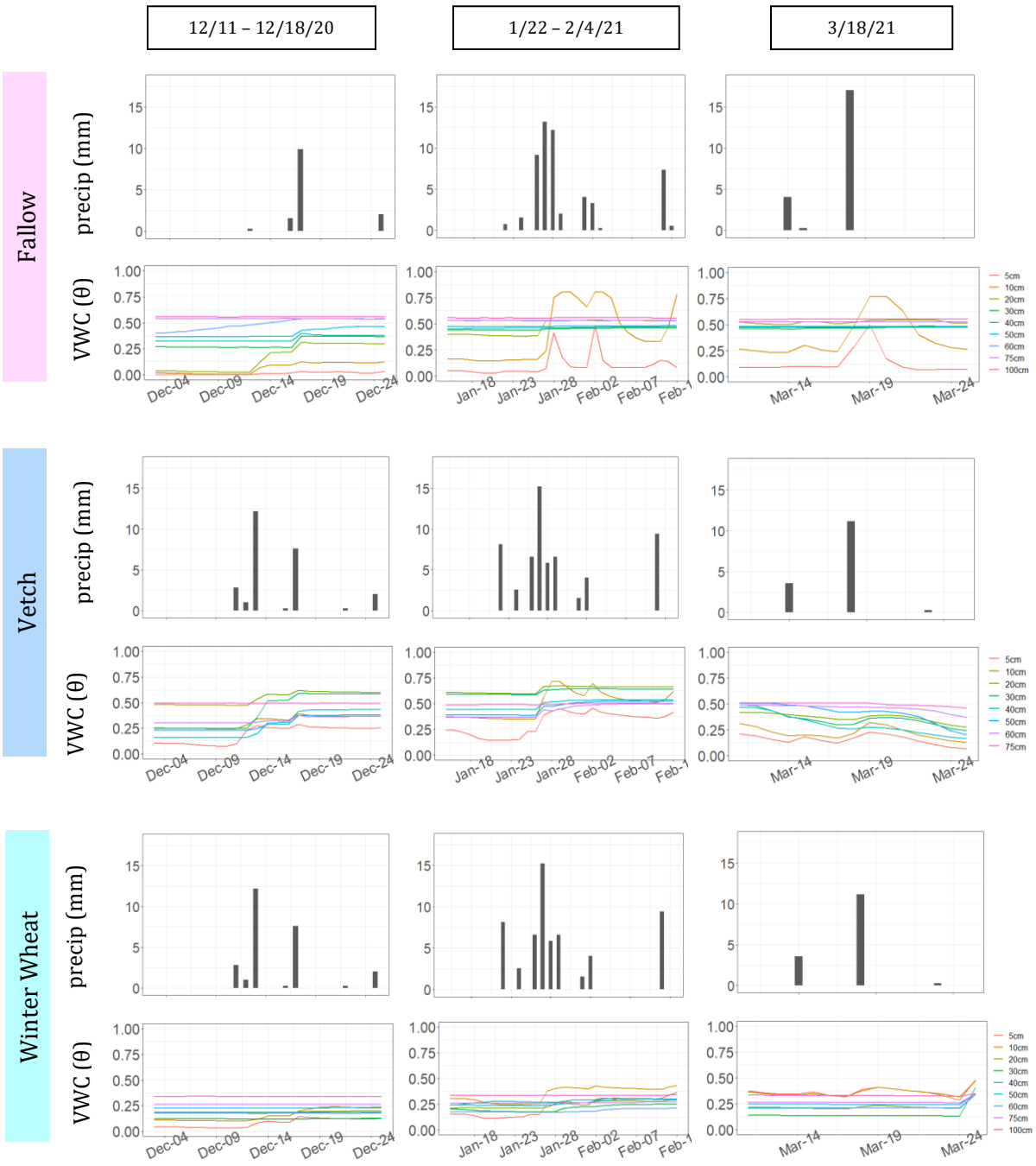

Fig 8: Volumetric water content (VWC, *θ*) by depth measured by TDR sensors, and precipitation collected from CIMIS stations at all sites for 3 major precipitation events.

Soil texture and plant water uptake may have influenced the magnitude of ΔS recorded by the TDR sensor in response to precipitation events. The observed ΔS in the winter wheat was lower than in the fallow and vetch sites after major precipitation events (Dec 15 and Feb 1) and remained lower until the irrigation event. High clay content soils (fallow and vetch) have a low hydraulic conductivity and sandy soils (winter wheat) have a higher hydraulic conductivity (Tsubo et al. 2015; IAEA 2008). Thus, clayey soils hold on to more water and may inhibit infiltration to lower depths, in our case past the range of the TDR sensor. Sandier soils facilitate higher rates of infiltration and drainage. The winter wheat crop may have had larger water uptake than the vetch contributing to lower ΔS.

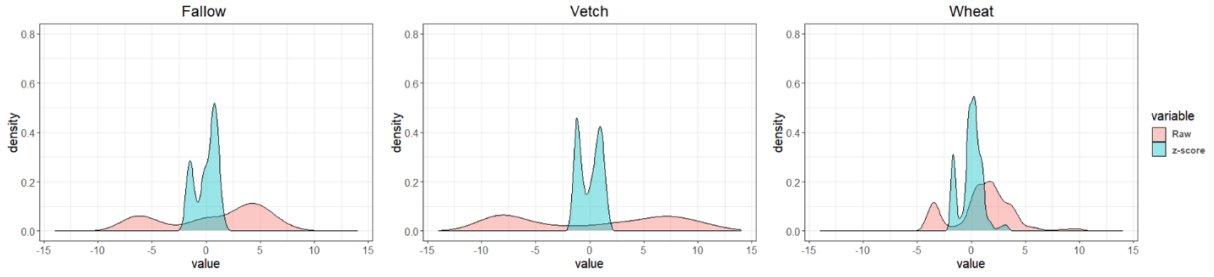

Fig 9: Daily, cumulative ΔS data distributions for raw and z-score data.

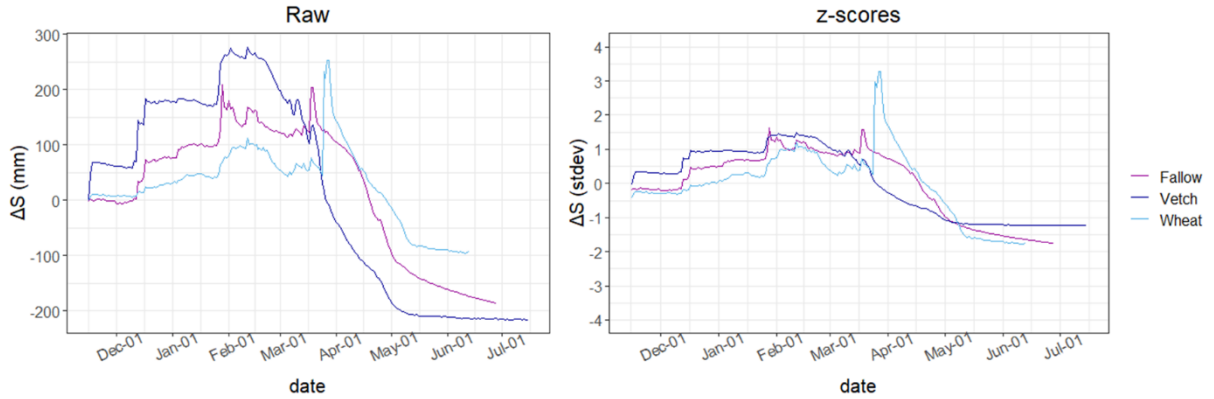

Fig 10: Cumulative raw and z-score ΔS data for entire season.

It is difficult to interpret ΔS from the TDR sensor for the last two months (June and July) of this study due to large amounts of noise detected at the fallow site and questionable readings at the vetch site that were most likely due to dry soil detaching from the sensor; the TDR sensor data from the winter wheat site had less detectable issues. Both the fallow and vetch TDR sensors measured soil moisture in high clay content soils >45% for most of their monitoring depth. The shrink-swell potential of clayey soils during drying likely interfered with TDR sensor readings contributing to these inconsistencies. Visible macropores in the form of large cracks in the soil surface were present in both the fallow and vetch sites and support this hypothesis. These macropores may have partially/fully exposed TDR sensor sensors to the atmosphere resulting in abnormally low readings compared to the soil cores at the end of the season (*Table 6*). The visual inspection of potential cracks in the winter wheat soil was more difficult sue to the dense, tall vegetation. *Table* 6 comparisons between the TDR sensor and soil cores are partially limited by availability of only one TDR sensor per field. Therefore, the comparisons are between the one point measured by the TDR sensor, and the average of 4 soil cores across sampling locations.

Field	End depth (m)	start		end	
		Core (mm)	TDR sensor (mm)	core (mm)	TDR sensor (mm)
Fallow	0.3	54.38	40.64	49.80	1.02
	0.6	136.73	162.56	134.93	54.10
	0.9	241.10	335.28	227.73	147.32
Vetch	0.3	67.71	45.31	27.94	8.89
	0.6	160.26	119.68	81.57	39.12
	0.9	268.27	258.00	162.75	1.54
Winter wheat	0.3	66.81	33.71	31.59	10.13
	0.6	127.94	96.77	72.40	39.10
	0.9	190.30	188.49	117.37	96.41

Table 6: Start and end of season cumulative depth of soil moisture (S) from soil cores (0.3 m increments) and TDR sensor (summed sensor depth readings corresponding to soil core depth increments).

At the end of the season vetch retained only 7% of fractional soil moisture from peak soil moisture from precipitation, significantly less than fallow, 36%, and winter wheat, 30% (*Fig 11*). Because of the large irrigation input, winter wheat held on to approximately the same percent of fractional soil moisture from precipitation as fallow. The irrigation input determined by the grower sufficiently matched the winter wheat's water demand, resulting in the soil water depletion equivalent to the fallow site. These results should be taken with caution considering the observed problems encountered with the TDR sensor in over estimating soil moisture when saturated and underestimating when dry at the end of the season. Fractional soil moisture may be more useful when calculated from a TDR sensor installed in non-clayey soils. Spatial variability in soil moisture observed from the sampled soil cores requires a closer look at these systems to determine the significance of these trends.

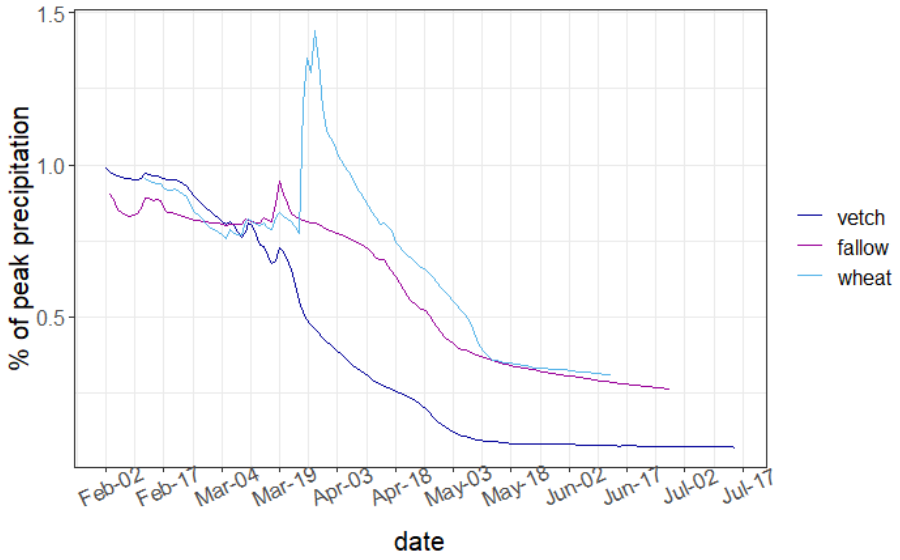

Fig 11: End of season fractional soil moisture, or percentage of soil moisture retained from peak soil moisture from precipitation.

Cumulative Water Budget Components

Averaged, daily cumulative *ΔS*, P, and I seasonal time series were compared (*Fig 12*). Across all sites, the TDR sensor responded to precipitation and irrigation events by recording increases in *ΔS*. However, both the fallow and vetch TDR sensors largely overestimated the magnitude of *ΔS* during high intensity precipitation events, recording magnitudes of *ΔS* greater than magnitudes of precipitation input for three identified events occurring on 12/11 – 12/18/20, 1/22-2/4/21, and 3/18/21. *ΔS* measured at the fallow site was 2.14 – 4.60 times more than recorded precipitation, and *ΔS* at the vetch site was 1.85 – 5.37 times more for identified events (*Table 7*). Because system outputs cannot be greater than inputs, the TDR sensor either inadequately measured *ΔS* or our measurement at one point in each field was an extremely insufficient representation of field scale *ΔS* and subsurface water dynamics. TDR sensor *ΔS* measured in the winter wheat field during precipitation

and irrigation events was also overestimated but not to the same degree as the fallow and vetch. *ΔS* measured at the winter wheat site was 0.82 – 2.10 times the amount of recorded precipitation (*Table 7*).

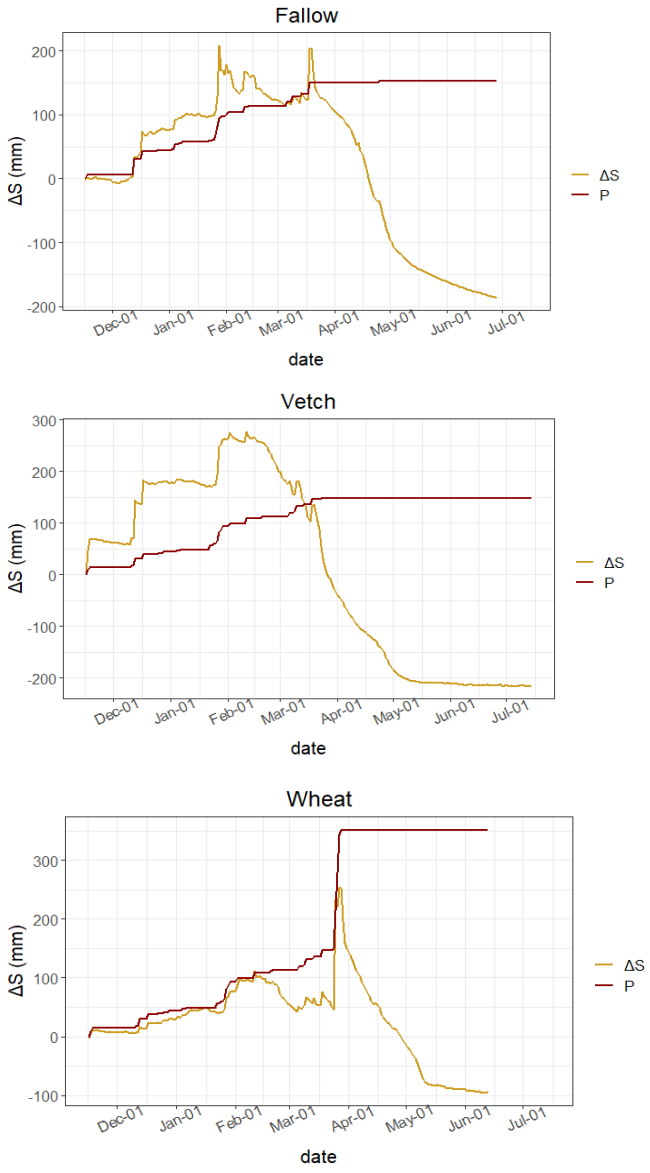

Fig 12: Averaged, daily cumulative change in soil moisture (*ΔS)*, precipitation (*P)*, and irrigation (*I*) for all sites.

	12/11 – 12/ 18/2020			1/22 – 2/4/21			3/18/21		
	P (mm)	ΔS (mm)	ΔS /P	P (mm)	ΔS (mm)	ΔS /P	P (mm)	ΔS (mm)	ΔS /P
Fallow	36.1	77.21	2.14	36.58	104.14	2.85	17.02	78.23	4.60
Vetch	23.88	128.3	5.37	50.04	92.46	1.85	11.43	39.12	3.42
Winter Wheat	23.88	19.56	0.82	50.04	54.61	1.09	11.43	23.88	2.10

Table 7: Comparison of measured TDR sensor ΔS to P for three precipitation events. ΔS /P represents the fraction of precipitation measured by TDR sensor ΔS (i.e., ΔS /P = 2 indicates that TDR sensor ΔS was 2 times more than recorded P for a particular event).

Differences in overestimations of TDR sensor ΔS between sites could be linked to soil type and heterogeneity. There was a greater overestimation of TDR sensor ΔS at the fallow and vetch sites than at the wheat site. Both fallow and vetch sites contain high clay content soils while the wheat site has no soil with clay content > 45%, which may account for differences in TDR sensor interferences. Another look at θ by depth for these events (*Fig 7*) confirms that both fallow and vetch TDR sensors measured greater increases in θ than wheat, with most change occurring in the top 0.3 m of the soil profile where fallow and vetch sites consist of high clay content soils (*Fig 4*). This indicates that clay content may have had an effect of TDR sensor measurements. Overestimation of ΔS in clayey soils has been linked to soil dielectric properties. Clay soils usually have higher bulk electrical conductivity and permittivity than sandy soils due to charged surfaces of clay particles surfaces (Gong et al. 2003). These soil properties tend to dampen the signal of TDR sensors and result in an overestimation in soil moisture (Stangl et al. 2009). While our findings align with the literature, more replications of this study in varying clay content soil is

needed to make a definitive conclusion on the affects of clay content on TDR sensor readings in winter cropped rice systems.

Seasonal Water Budgets

Seasonal values of WBCs are summarized in *Table 8* and *Fig 13.* The winter of 2020-2021 was dry compared to an average water year in Sacramento Valley; all sites received comparable seasonal inputs from precipitation of an average of 149.61 mm (California Department of Water Resources et al. 2021). The winter wheat field received an irrigation input of 224.96 mm which more than doubled its total inputs compared to the vetch and fallow sites. Average ΔS across sampling locations collected from soil cores was -34.80, -202.69, and --60.20 mm while ΔS from the single TDR sensor location was -186.96, -181.61, and -91.44 mm for fallow, vetch, and winter wheat respectively. Seasonal *ETc* values calculated as the residual of the water budget were 182.46, 325.57, and 422.15 mm using the soil cores and 339.36, 364.34, 464.23 mm using the TDR sensor for the fallow, vetch, and winter wheat sites respectively. Additional years of this study will aid in confirming sources of error in seasonal water budgets.

	P (mm)	I (mm)	ΔS TDR sensor (mm)	ΔS Cores (mm)	ETc TDR sensor (mm)	ETc Cores (mm)	ET_o CIMIS (mm)
Fallow	152.40		-186.96	-34.80	339.36	182.46	768
Vetch	147.83		-181.61	-202.69	364.34	325.57	900-936
Winter wheat	147.83	224.96	-91.44	-60.20	464.23	422.15	687-806

Table 8: Seasonal water budget components (WBCs) for all sites including precipitation (P), irrigation (I), soil water storage (ΔS) from soil cores and TDR sensor, and crop evapotranspiration (ETc) estimated as the residual of the water budgets using soil cores and TDR sensor ΔS measurements.

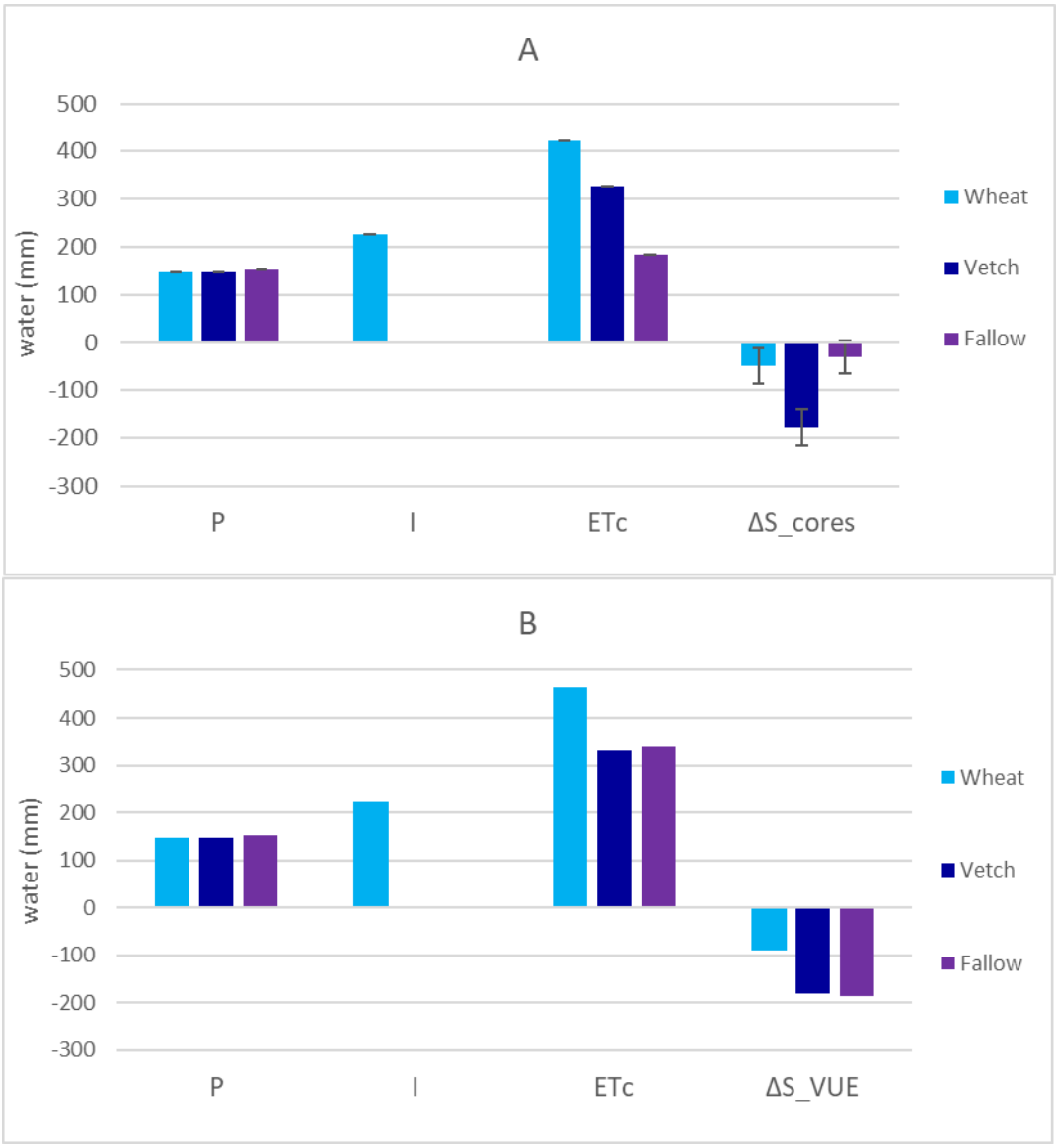

Fig 13: Seasonal water budgets for all sites where ETc is estimated as the residual of water budgets using *ΔS* measured from soil cores (A) and TDR sensor (B).

Application and Limitations

Specifically in dry years, many rice growers are interested in tradeoffs between maintaining agroecosystems, such as winter crops, and fallowing to pursue water sales. Our present findings are representative of an extremely dry water year. Growers interested in providing nesting habitat for migratory birds while simultaneously selling

water may be interested in pursuing a either an irrigated or non-irrigated winter crop. Winter crops harvested for profit that need to reach maturity and maintain quality, such as winter wheat, would likely require additional irrigation inputs to maintain growth as temperatures increase without precipitation. Winter crops grown for the purpose of habitat creation and soil health could still provide these benefits without irrigation inputs.

The non-irrigated winter crop in this study (vetch) had less seasonal consumptive use (325.57 mm) than the irrigated, harvested for profit, winter crop (winter wheat) (422.15 mm). Both winter crops had significantly smaller *ETc* than rice (May-Sept, 889-1,143 mm) and consequently have the potential to provide bird habitat with water left over to sell/transfer (Lal et al. 2012; Wong et al. 2021). Furthermore, water sales are primarily offered during the summer which for an extended winter crop growing season would be May, June, and July. This means that only the last months of the winter crop growing season would be considered in calculating the crops summer consumptive use, increasing water quantities available for sale/transfer and the attractiveness of this management practice to growers. In-situ ETc measurements at a monthly time step are needed to determine exact quantities during this summertime period critical for bird nesting. Calculation of *ETc* in this research was limited by the lack of directly measured deep percolation, sub-lateral flow, small runoff quantities not captured by our monitoring weir, TDR sensor error, and precipitation measured off site.

As seen in this study, non-irrigated winter crops could deplete the soil profile more than fallowed land during drought periods by drawing water from lower depths of the soil profile. An earlier termination of non-irrigated winter crops may allow for soil health benefits during the cool season to be better retained through the summer by reducing soil

moisture depletion from crop *ETc* as temperatures rise. The fallow site higher rates of decline in ΔS after precipitation events than both vetch and winter wheat, indicating a higher potential to retain soil moisture in winter-cropped sites. This trend has also been observed during average and wet water years where winter crops have been shown to improve soil health, reduce runoff and erosion, and promote infiltration and water retention; benefits that may be more significant than, or equal to, fallowing during non-drought years (Devincentis 2020; Colla et al. 2000). The tradeoff between preserving soil moisture by early termination of conserving bird habitat is a decision that individual growers should consider when thinking about what is best for their farm. Our study results are aimed to inform these decisions by quantifying potential winter crop water use. It may be helpful information when considering farm management options during different water years (wet, moderate, dry).

The results from this study are useful for conservationists and water managers working in systems with high clay content soils for several reasons. In dry years, multi-depth downhole TDR sensors may be accurate in measuring relative changes in ΔS at depth, but less accurate in measuring absolute magnitude. This is an important distinction as taxongrowers work towards better quantifying their water use and loss in adapting to droughts and climate associated water challenges. Overestimated ΔS during precipitation events made determination of ΔS difficult and was more prominent in clay soils, likely from swelling interferences. Additionally, the TDR sensor did not perform accurately in clayey soils during the particularly dry, hot conditions of our monitoring season as soil cracked and separated from the sensor producing noise.

Also, site specific soil calibration was laborious and minimally effective since soil from multiple depths of the soil profile were mixed for the calibration process and not representative of the soils at individual sensor depths during the measuring season. Following years of this study may perform in-situ calibrations by manually collecting soil cores near TDR sensors during different times of the year and comparing core VWC to TDR sensor reading and each sensor depth. This method would better capture the season's soil moisture range and profile. Monitoring TDR sensor data and reinstalling if soil detachment or noise is detected could improve the chances for better soil moisture monitoring, but risks consistency in soil physical properties surrounding the sensor. New cracks can always form after reinstalment and the challenge of preserving soil sensor contact remains. However, the ease of the TDR sensor makes it a useful tool when conditions permit.

The diversity of our field sites are representative of inherent variability in the Sacramento Valley's agricultural systems, and it's what makes field-based applied research so challenging. To best compare winter cropping treatments to a control, it would be optimal for the fallow site to be in the same proximity as the vetch and winter wheat. For the 2021 water year, both regions received similar precipitation patterns which is not always the case but beneficial for treatment comparisons. Additionally, soil variability between sites and at a field scale required meticulous analysis in an effort to explain and draw broader conclusions about the studied systems.

The results and lessons learned from this research can help address these limitations during future years of this study. Locating study sites closer to each other would decrease pedoclimatic differences between sites, however intrinsic variability in

farm management, cropping history, and type of winter crop are unavoidable. Differences in soil texture and/or physical properties within a field among sampling locations are potential sources of variability in ΔS at each site, however soil nutrients, organic matter, topography, and crop uniformity/physiology also affect ΔS and were not measured in this study. There are infinite combination of soil texture and bulk density, each having unique soil water dynamics. Increasing sampling size of soil cores at the start and end of the season, and installing multiple TDR sensors, could provide a better representation of field scale ΔS by better representing field heterogeneity. Additionally, multiple mid-season soil cores analyzed for S could provide insight to when the TDR sensor may be experiencing inconsistencies.

Conclusions

The purpose of this study was twofold; first, to assess the application of field scale water budget models for informing agricultural water management decisions, and second, to review the application of the TDR sensor TDR sensor in measuring soil moisture in high clay content soils. In our case study of winter-cropped, fallowed rice fields in the Sacramento Valley seasonal *ETc* was calculated from water budgets and soil water dynamics were monitored at a daily time step. We found that winter crops use less water than rice crops normally planted during the summer season; therefore, the winter crop growing season could be extended to provide bird habitat during critical nesting periods in late spring/early summer with remaining water being sold/transferred during dry years.

This research confirm findings from the literature that overestimation of soil moisture in saturated conditions and underestimation in dry conditions is a major limitation of applying measurements from the TDR sensor TDR sensor to water budget

models (IAEA 2008; Stangl et al. 2009). This is especially true in clayey soils, where shrink-swell potential is high and increases the probability of soil separating from the sensor. The TDR sensor could be useful in understanding how water moves through the soil profile in non-clayey soils and further research should be done connecting crop water use in the root zone to soil water movement through different soil profile layers and textures.

References

Abdullah, N. H.H., N. W. Kuan, A. Ibrahim, B. N. Ismail, M. R.A. Majid, R. Ramli, and N. S. Mansor. 2018. “Determination of Soil Water Content Using Time Domain Reflectometer (TDR) for Clayey Soil.” *AIP Conference Proceedings 2020*, no. October. https://doi.org/10.1063/1.5062642.

Baker, Dirk V, and Campbell Scientific. 2021. “Soil-Specific Calibration Procedure for Volumetric Water Content Sensors.” Campbell Scientific.

Baldocchi, Dennis, David Dralle, Chongya Jiang, and Youngryel Ryu. 2019. “How Much Water Is Evaporated Across California? A Multiyear Assessment Using a Biophysical Model Forced With Satellite Remote Sensing Data.” *Water Resources Research* 55 (4): 2722–41. https://doi.org/10.1029/2018WR023884.

Blake, George R. 2008. “Particle Density.” *Encyclopedia of Soil Science. Encyclopedia of Earth Sciences Series*. https://doi.org/10.1007/978-1-4020-3995-9_406.

Boretti, Alberto, and Lorenzo Rosa. 2019. “Reassessing the Projections of the World Water Development Report.” *Npj Clean Water* 2 (1). https://doi.org/10.1038/s41545-019-0039-9.

Bunn, Stuart E., and Angela H. Arthington. 2002. “Basic Principles and Ecological Consequences of Altered Flow Regimes for Aquatic Biodiversity.” *Environmental Management* 30 (4): 492–507. https://doi.org/10.1007/s00267-002-2737-0.

California Department of Water Resources and Bureau of Reclamation. 2019. “Technical Information for Preparing Water Transfer Proposals (Water Transfer White Paper) Information for Parties Preparing Proposals for Water Transfers Requiring Department of Water Resources or Bureau of Reclamation Approval.”

California Department of Water Resources, and California Natural Resources Agency. 2021. “Water Year 2021 : An Extreme Year.”

California State Water Resources Control Board. 1999. “A Guide to Water Transfers (Draft).”

Central Valley Bird Club. 2017. “Sacramento County Breeding Bird Atlas.”

http://www.cvbirds.org/birding-resources/sacramento-county-breeding-bird-atlas/.

Chertkov, V. Y. 2012. “Physical Modeling of the Soil Swelling Curve vs. the Shrinkage Curve.” *Advances in Water Resources* 44: 66–84. https://doi.org/10.1016/j.advwatres.2012.05.003.

Childs, Nathan. 2021. “Rice Outlook.” *Economic Research Service, USDA*.

CIMIS. 2021. “The California Irrigation Management Information System.” https://doi.org/10.1007/BF02854009.

Colla, G., J. P. Mitchell, B. A. Joyce, L. M. Huyck, W. W. Wallender, S. R. Temple, T. C. Hsiao, and D. D. Poudel. 2000. “Soil Physical Properties and Tomato Yield and Quality in Alternative Cropping Systems.” *Agronomy Journal* 92: 924–32. https://doi.org/10.2134/agronj2000.925924x.

Devincentis, Alyssa. 2020. “Scales of Sustainable Agricultural Water Management.” *Journal of Chemical Information and Modeling*.

Douville, Hervé, Krishnan Raghavan, James Renwick, Richard P. Allan, Paola A. Arias, Mathew Barlow, Ruth Cerezo-Mota, et al. 2021. “Water Cycle Changes.” *Climate Change 2021: The Physical Science Basis. Contribution of Working Group I to the Sixth Assessment Report of the Intergovernmental Panel on Climate Change*. https://doi.org/10.21513/2410-8758-2017-2-13-25.

Frayer, W.E., Dennis D. Peters, and H. Ross Pywell. 1989. “Wetlands of the California Central Valley: Status and Trends 1939-1980s.” Portland, OR.

Gochis, David J, and Richard H Cuenca. 2000. “Plant Water Use and Crop Curves for Hybrid Poplars.” *Journal of Irrigation and Drainage Engineering* 126 (4): 206–14.

Gomboš, M, and A Tall. 2012. “Soil Clay Fraction Impact on Coefficient of Linear Extensibility,” no. 14.

Gong, Yuanshi, Qiaohong Cao, and Zongjia Sun. 2003. “The Effects of Soil Bulk Density, Clay Content and Temperature on Soil Water Content Measurement Using Time-Domain Reflectometry.” *Hydrological Processes* 17: 3601–14. https://doi.org/10.1002/hyp.1358.

Grossman, R.B., and T.G. Reinsch. 2002. “Bulk Density and Linear Extensibility.” In *Methods of Soil Analysis: Part 4 Physical Methods*, edited by Jacob H. Dane and G. Clarke Topp, 201–28.

Hanak, Ellen, Jay Lund, Barton Thompson, W. Bowman Cutter, Brian Gray, David Houston, Richard Howitt, et al. 2019. “Water and the California Economy.” *California at War*, 147–77. https://doi.org/10.2307/j.ctvg5bt1b.9.

Hardie, Marcus. 2020. “Review of Novel and Emerging Proximal Soil Moisture Sensors for Use in Agriculture.” *Sensors* 20. https://doi.org/10.3390/s20236934.

Hashim, Roslan, and Agus Setyo Muntohar. 2006. “Swelling Rate of Expansive Clay Soils.” *Expansive Soils: Recent Advances in Characterization and Treatment*, no. January 2006. https://doi.org/10.1201/9780203968079.ch11.

Healy, Richard W., Thomas C. Winter, James W. LaBaugh, and O.L. Franke. 2007. “Water Budgets : Foundations for Effective Water-Resources and Environmental Management.” *U.S. Geological Survey Circular* 1308.

Hue, Gabriel T. La. n.d. “Water Management for Improved Agronomic and Environmental Performance in California Rice By GABRIEL THOMAS LA HUE Submitted in Partial Satisfaction of the Requirements for the Degree of DOCTOR OF PHILOSOPHY in Soils and Biogeochemistry in the OFFICE OF GR.”

IAEA. 2008. “Field Estimation of Soil Water Content: A Practical Guide to Methods, Instrumentation and Sensor Technology.” *Training Course Series 30*. https://doi.org/10.2489/jswc.64.4.116a.

Iglesias, Ana, and Luis Garrote. 2015. “Adaptation Strategies for Agricultural Water Management under Climate Change in Europe.” *Agricultural Water Management* 155: 113–24. https://doi.org/10.1016/j.agwat.2015.03.014.

Johnson, Renee, and Betsy A Cody. 2015. “California Agricultural Production and Irrigated Water Use.”

Joyce, B a, W W Wallender, J P Mitchell, L M Huyck, S R Temple, P N Brostrom, and T C Hsiao. 2002. “Infiltration and Soil Water Storage Under Winter Cover Cropping in California’s Sacramento Valley.” *Society* 45 (2): 315–26.

Kelleners, T. J., M. S. Seyfried, J. M. Blonquist, J. Bilskie, and D. G. Chandler. 2005. “Improved Interpretation of Water Content Reflectometer Measurements in Soils.” *Soil Science Society of America Journal* 69: 1684–90. https://doi.org/10.2136/sssaj2005.0023.

Lal, Deepak, Byron Clark, Thad Bettner, Bryan Thoreson, and Richard Snyder. 2012. “Rice Evapotranspiration Estimates and Crop Coefficients in Glenn-Colusa Irrigation District, Sacramento Valley, California.” *USCID Water Management Conference Proceedings, Austin, California, USA*, no. April: 145–56.

LaRose, Joe, and Rob Myers. 2018. “Cover Crop Facts.”

Ledieu, J., P. De Ridder, P. De Clerck, and S. Dautrebande. 1986. “A Method of Measuring Soil Moisture by Time-Domain Reflectometry.” *Journal of Hydrology* 88 (3–4): 319–28. https://doi.org/10.1016/0022-1694(86)90097-1.

Li, Jie, David W Smith, Stephen G Fityus, and Daichao Sheng. 2003. “Numerical Analysis of Neutron Moisture Probe Measurements.” *International Journal of Geomechanics* September.

Linquist, Bruce, Richard Snyder, Frank Anderson, Luis Espino, Guglielmo Inglese, Serena Marras, Ruben Moratiel, et al. 2015. “Water Balances and Evapotranspiration in Water- and Dry-Seeded Rice Systems.” *Irrigation Science* 33 (5): 375–85. https://doi.org/10.1007/s00271-015-0474-4.

Lokemoen, John T., and A. Beiser, Julia. 1997. “Bird Use and Nesting in Conventional , Minimum-Tillage , and Organic Cropland.” *The Journal of Wildlife Management* 61 (3): 644–55.

Malongweni, Siviwe Odwa, Yasutaka Kihara, Kuniaki Sato, Takeo Tokunari, Tabhorbayar Sobuda, Kaya Mrubata, and Tsugiyuki Masunaga. 2019. “Impact of Agricultural Waste on

the Shrink–Swell Behavior and Cracking Dynamics of Expansive Soils." *International Journal of Recycling of Organic Waste in Agriculture* 8 (4): 339–49. https://doi.org/10.1007/s40093-019-0265-7.

Mount, Jeffrey, and Ellen Hanak. 2019. "Water Use in California: Just the Facts." *PPIC Water Policy Center*.

Nocco, Mallika A., George J. Kraft, Steven P. Loheide, and Christopher J. Kucharik. 2018. "Drivers of Potential Recharge from Irrigated Agroecosystems in the Wisconsin Central Sands." *Vadose Zone Journal* 17 (1): 170008. https://doi.org/10.2136/vzj2017.01.0008.

NRCS. 2021. "Web Soil Survey: Marcum Clay Loam."

Pan, Xicai, Warren Helgason, Andrew Ireson, and Howard Wheater. 2017. "Field-Scale Water Balance Closure in Seasonally Frozen Conditions." *Hydrology and Earth System Sciences* 21 (11): 5401–13. https://doi.org/10.5194/hess-21-5401-2017.

Parker, J.C., D.F. Amos, and D.L. Kaster. 1977. "An Evaluation of Several Methods of Estimating Soil Volume Change." *Soil Science Society of America Journal* 41: 1059–64.

Pettygrove, G.S., and J.F. Williams. 1996. "Nitrogen-Fixing Covercrops for California Rice Production."

Safeeq, Mohammad, Ryan R Bart, Norman F Pelak, Peter Hartsough, David N Dralle, and Joseph W Wagenbrenner. 2021. "How Realistic Are Water-Balance Closure Assumptions ? A Demonstration from the Southern Sierra Critical Zone Observatory and Kings River Experimental Watersheds Study Area," no. April: 1–16. https://doi.org/10.1002/hyp.14199.

Stangl, R., G. D. Buchan, and W. Loiskandl. 2009. "Field Use and Calibration of a TDR-Based Probe for Monitoring Water Content in a High-Clay Landslide Soil in Austria." *Geoderma* 150: 23–31. https://doi.org/10.1016/j.geoderma.2009.01.002.

Stanton, J.S., S.L. Qi, D.W. Ryter, S.E. Falk, N.A. Houston, S.M. Peterson, and S.C. Westenbroek, S.M., Christenson. 2011. "Selected Approaches to Estimate Water-Budget Components of the High Plains , 1940 through 1949 and 2000 through 2009." *U.S.*

Geological Survey Scientific Investigations Report.

Strum, Khara M., Matthew E. Reiter, C. Alex Hartman, Monica N. Iglecia, T. Rodd Kelsey, and Catherine M. Hickey. 2013. “Winter Management of California’s Rice Fields to Maximize Waterbird Habitat and Minimize Water Use.” *Agriculture, Ecosystems and Environment* 179: 116–24. https://doi.org/10.1016/j.agee.2013.08.003.

Thorup-kristensen, Kristian, Montserrat Salmeron Cortasa, and Ralf Loges. 2009. “Winter Wheat Roots Grow Twice as Deep as Spring Wheat Roots , Is This Important for N Uptake and N Leaching Losses ?” *Plant Soil* 322: 101–14. https://doi.org/10.1007/s11104-009-9898-z.

Topp, G. Clarke, and W. Daniel Reynolds. 1998. “Time Domain Reflectometry: A Seminal Technique for Measuring Mass and Energy in Soil.” *Soil and Tillage Research* 47 (1–2): 125–32. https://doi.org/10.1016/S0167-1987(98)00083-X.

Tsubo, Mitsuru, Shu Fukai, Jayampathi Basnayake, To Phuc Tuong, Mitsuru Tsubo, Shu Fukai, Jayampathi Basnayake, and To Phuc Tuong. 2015. “Effects of Soil Clay Content on Water Balance and Productivity in Rainfed Lowland Rice Ecosystem in Northeast Thailand Effects of Soil Clay Content on Water Balance and Productivity in Rainfed Lowland Rice Ecosystem in Northeast Thailand” 1008. https://doi.org/10.1626/pps.10.232.

Verstraeten, Willem W., Frank Veroustraete, and Jan Feyen. 2008. “Assessment of Evapotranspiration and Soil Moisture Content across Different Scales of Observation.” *Sensors* 8 (1): 70–117. https://doi.org/10.3390/s8010070.

Wan, Zhanming, Ke Zhang, Xianwu Xue, Zhen Hong, Yang Hong, and Jonathan J. Gourley. 2015. “Water Balance-Based Actual Evapotranspiration Reconstruction from Ground and Satellite Observations over the Conterminous United States.” *Water Resour. Res.* 51: 6485–6499. https://doi.org/doi:10.1002/2015WR017311.

Widomski, Marcin K., Witold Stępniewski, Rainer Horn, Andrzej Bieganowski, Lucjan Gazda, Małgorzata Franus, and Małgorzata Pawłowska. 2015. “Shrink-Swell Potential, Hydraulic

Conductivity and Geotechnical Properties of Clay Materials for Landfill Liner Construction." *International Agrophysics* 29 (3): 365–75. https://doi.org/10.1515/intag-2015-0043.

Wong, A. J., Y. Jin, J. Medellín-Azuara, K. T. Paw U, E. R. Kent, J. M. Clay, F. Gao, et al. 2021. "Multiscale Assessment of Agricultural Consumptive Water Use in California's Central Valley." *Water Resources Research* 57 (9): 1–28. https://doi.org/10.1029/2020WR028876.

Zeleke, Ketema Tilahun, and Leonard John Wade. 2012. "Evapotranspiration Estimation Using Soil Water Balance, Weather and Crop Data." In *Evapotranspiration - Remote Sensing and Modeling*, 41–58. IntechOpen. https://doi.org/10.5772/725.

Appendix 1:

Calibration curves for TDR sensor installed at the vetch site (A) and fallow site (B). The TDR sensor at the winter wheat site was not calibrated because there was no soil with clay content >45%.

A

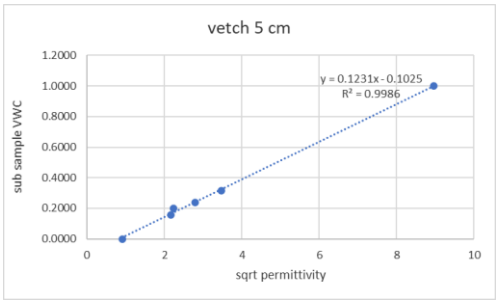

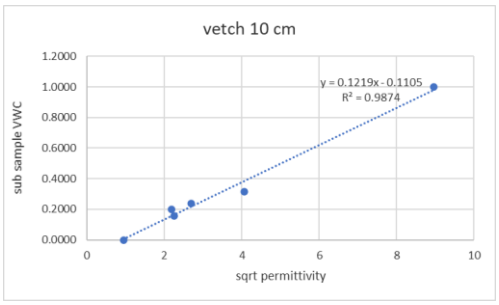

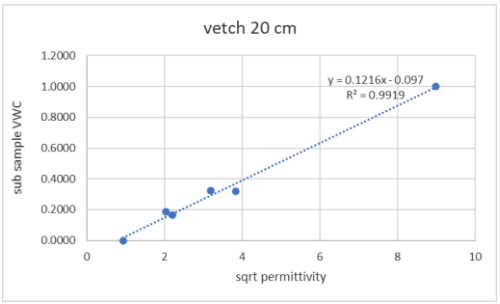

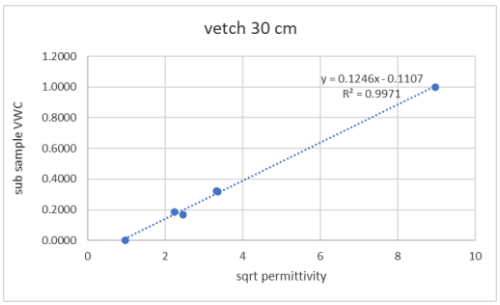

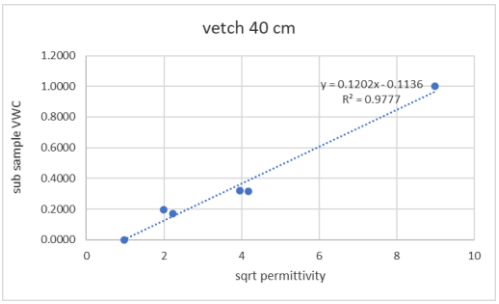

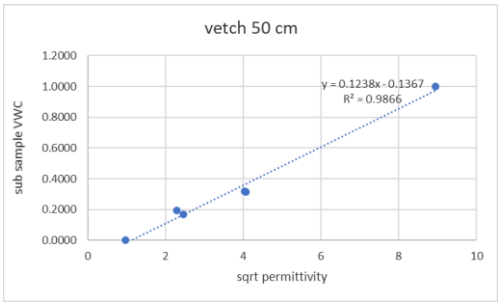

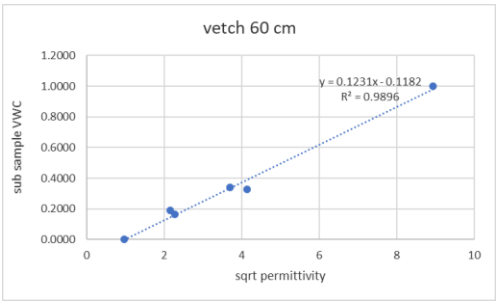

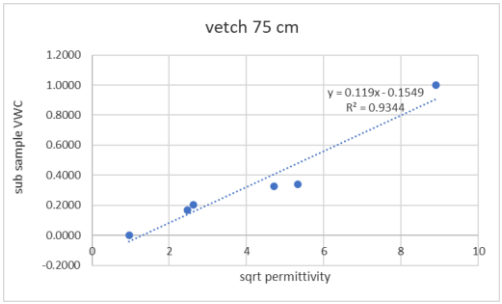

B

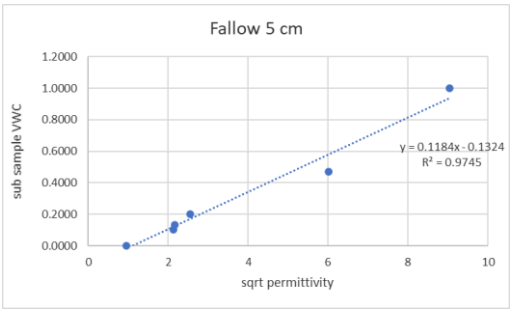

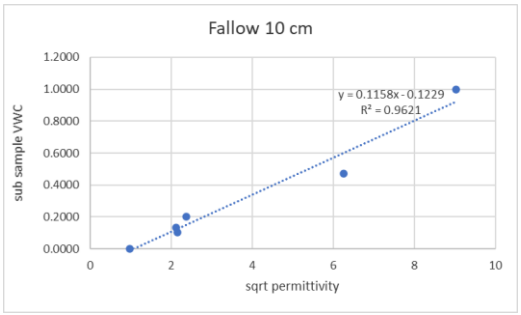

Appendix 2:

Soil texture obtained from soil core particle analysis at the start of the season.

	depth (m)	Sand %	Silt %	Clay %
Fallow	0.3	22.20	28.20	49.60
	0.6	22.40	26.20	51.40
	0.9	37.60	28.70	33.70
	1.2	45.33	30.00	24.67
	1.5	49.67	28.67	21.67
	1.8	53.67	25.33	21.00
	2.1	53.67	25.67	20.67
	2.4	58.33	23.00	18.67
Vetch	0.3	18.00	28.40	53.60
	0.6	16.40	28.30	55.30
	0.9	21.70	31.00	47.30
	1.2	40.00	36.33	23.67
	1.5	40.00	44.67	15.33
	1.8	45.67	42.67	11.67
	2.1	53.00	40.00	7.00
	2.4	58.00	36.00	6.00
Wheat	0.3	37.33	38.67	24.00
	0.6	51.83	23.67	24.50
	0.9	59.33	18.33	22.33
	1.2	52.83	26.33	20.83
	1.5	47.00	28.67	24.33
	1.8	44.33	28.00	27.67
	2.1	46.00	26.67	27.33
	2.4	51.50	22.33	26.17

Appendix 3:

Bulk density (ρ_b) and porosity (n) calculated from soil cores taken during mid-season and end of season.

		mid-season		end of season		change, end-mid	
	End depth (m)	ρ_b $(\frac{g}{cm^3})$	n (cm^3/ cm^3)	ρ_b $(\frac{g}{cm^3})$	n (cm^3/ cm^3)	$\Delta\rho_b$ $(\frac{g}{cm^3})$	Δn (cm^3/ cm^3)
Fallow	0.3	0.95	0.64	1.46	0.45	0.51	-0.19
	0.6	1.21	0.54	1.64	0.38	0.42	-0.16
	0.9	1.25	0.53	1.63	0.38	0.38	-0.14
Vetch	0.3	0.97	0.63	1.27	0.52	0.30	-0.11
	0.6	1.42	0.57	1.49	0.44	0.35	-0.13
	0.9	1.17	0.56	1.48	0.44	0.31	-0.12
Winter wheat	0.3	1.08	0.59	1.37	0.48	0.28	-0.11
	0.6	1.21	0.55	1.67	0.37	0.47	-0.18
	0.9	1.41	0.47	1.82	0.31	0.41	-0.15